MASTER OF SCIENCE IN ELECTRICAL AND ELECTRONIC ENGINEERING

Development of Generalized Unified Power Flow Controller (GUPFC) based Damping Controller for the Enhancement of Small Signal Stability of SMIB System

Department of Electrical and Electronic Engineering
Islamic University of Technology (IUT)
Board Bazar, Gazipur-1704, Bangladesh
October, 2019

Development of Generalized Unified Power Flow Controller (GUPFC) based Damping Controller for the Enhancement of Small Signal Stability of SMIB System

by

Md. Maksudur Rahman

MASTER OF SCIENCE

IN

ELECTRICAL AND ELECTRONIC ENGINEERING

Department of Electrical and Electronic Engineering
Islamic University of Technology (IUT)
Board Bazar, Gazipur-1704, Bangladesh
October, 2019

CERTIFICATE OF APPROVAL

The thesis titled "**Development of Generalized Unified Power Flow Controller (GUPFC) based Damping Controller for the Enhancement of Small Signal Stability of SMIB System**" submitted by Md. Maksudur Rahman, St. No. 152605 of Academic Year 2015-2016 has been found as satisfactory and accepted as partial fulfillment of the requirement for the Degree **of MASTER OF SCIENCE IN ELECTRICAL AND ELECTRONIC ENGINEERING** on 28 October, 2019.

Board of Examiners:

1.

_____

Dr. Ashik Ahmed — Chairman
Associate Professor, (Supervisor)
Department of Electrical and Electronic Engineering
Islamic University of Technology (IUT), Gazipur.

2.

_____

Dr. Md. Ruhul Amin — Member
Professor and Head,
Department of Electrical and Electronic Engineering
Islamic University of Technology (IUT), Gazipur.

3.

_____

Dr. Md. Fokhrul Islam — Member
Associate Professor,
Department of Electrical and Electronic Engineering
Islamic University of Technology (IUT), Gazipur.

4.

_____ Member (External)

Dr. Md. Raju Ahmed
Professor,
Department of Electrical and Electronic Engineering
Dhaka University of Engineering & Technology (DUET), Gazipur

Declaration of Candidate

It is hereby declared that this thesis report or any part of it has not been submitted elsewhere for the award of any Degree or Diploma.

_____	_____
Dr. Ashik Ahmed	Md. Maksudur Rahman
Associate Professor,	Student No.:152605
Electrical and Electronic Engineering Department,	Academic Year: 2015-16
Islamic University of Technology (IUT).	Date:
Date:	

Dedicated to

My respected Parents and adorable Wife

"Without whom none of my success would be possible"

Table of Contents

Page No.

Chapter 3: Methodology

Chapter 4: Analysis of GUPFC

Chapter 5: Conclusion and Recommendations for Future Works

List of Figures

List of Tables

List of Abbreviation of Technical Terms

FACTS	Flexible AC Transmission Systems
LFO	Low Frequency Oscillation
SSSSC	Static Synchronous Series Compensator
STATCOM	Static Synchronous Compensator
GUPFC	Generalized Unified Power Flow Controller
UPFC	Unified Power Flow Controller
IPFC	Interline Power Flow Controller
VSC	Voltage Source Converter
PSO	Particle Swarm Optimization
DE	Differential Evolution
GWO	Grey Wolf Optimization
SMIB	Single Machine Infinite Bus
EM	Electromechanical Mode
DAE	Differential Algebraic Equation
POD	Power Oscillation Damping
ODE	Ordinary Differential Equation
PI	Proportional Integral
SVC	Static Var Compensator
GTO	Gate Tun-off Thyristor
IGBT	Insulted Gate Bipolar Thyristor
TCSC	Thyristor Controlled Series Compensator
FPA	Flower Pollination Algorithm
PSS	Power System Stabilizer
RAM	Random Access Memory
QPSO	Quantum Particle Swarm Optimizer

Nomenclature

δ_A, δ_B	Boosting converter phase angle of GUPFC
δ_E	Excitation converter phase angle of GUPFC
δ, ω	Rotor speed and angle
ω_0	Base speed
C_{dc}	dc link capacitance of GUPFC
D, M	Machine damping and inertia co-efficient
$\acute{E_q}$	Internal voltage behind q-axis transient reactance
E_{fd}	Equivalent excitation voltage
I_T	Generator output current
$I_{Ad,}I_{Aq}$	A branch d - q axis boosting current for GUPFC
$I_{Bd,}I_{Bq}$	B branch d - q axis boosting current for GUPFC
$I_{Ed,}I_{Eq}$	d – q axis excitation current for GUPFC
K	Gain of damping controller
$K_{A,}T_A$	Gain and time constant of generator excitation system
$m_{A,}m_B$	Amplitude modulation ratio of boosting converters of GUPFC

m_E	Amplitude modulation ratio of excitation converter of GUPFC
$P_{e,}P_m$	Electrical output and mechanical input power
$T_{1,}T_3$	Lead time constant of Lead-Lag controller
$T_{2,}T_4$	Lag time constant of Lead-Lag controller
T_e	Electromagnetic Torque
T_s, K_s	Gain and time constant for filter
T_w	Washout time constant
$T_{d0}^{\acute{}}$	Open circuit d-axis transient time constant
V_b	Infinite bus voltage magnitude
V_T	Generator terminal voltage magnitude
V_{dcref}	dc regulator reference voltage
X_A, X_B	Boosting transformer reactance of GUPFC
$X_d^{\acute{}}$	d - axis transient reactance of generator
X_d, X_q	d - q *axis steady-state reactance of generator*
X_E	Excitation transformer reactance
X_{AV}, X_{BV}	Reactance of transmission line

ACKNOWLEDGEMENT

First and foremost all the praise is paid to the Almighty, the most kind Allah for keeping me alive and able, giving me the knowledge, ability to think and for helping me to successfully finish this thesis.

The author express his whole hearted deep gratitude, indebtedness appreciation to his honorable teacher, respected supervisor Dr. Ashik Ahmed for his continuous assistance, inspiration, guidance and valuable suggestions throughout the period of research.

The author would like to extend his deep sense of gratitude to all of the respective teachers of the Department of Electrical and Electronic Engineering, IUT for their valuable suggestions, cooperation and best wishes.

Finally, the author acknowledges that this work would be almost impossible to carry out successfully without the inspirations from his parents as they give moral support, optimistic encouragement throughout the research work.

Md. Maksudur Rahman

October, 2019

ABSTRACT

Low frequency oscillation is one of the major concerns for reliable operation of power system, which occurs due to the failure of the rotor to supply sufficient damping torque to compensate the imbalance between mechanical input and electrical output of a conventional power system. In this research work, a third generation FACTS device named Generalized Unified Power Flow Controller (GUPFC) based damping controller has been adopted in order to investigate its effect for mitigating low frequency oscillation. To perform a comprehensive study as well as to find the effectiveness of the designed damping controller, two conventional controllers such as PI and Lead-Lag controller have been integrated for an Single Machine Infinite Bus (SMIB) power system and test their performances on a separate manner. Later, since improper modulation of gain and time constant parameters of these two above mentioned controllers may lead to sub-optimal result, three different optimization algorithms such as Gray Wolf Optimization (GWO), Differential Evolution (DE) optimization, and Particle Swarm Optimization (PSO) have been adopted to tune these gains and time constants. Then, to study the efficacy of these optimizers, time domain simulations as well as quantitative analysis have been performed to find out the most suitable optimizer for each of the above controllers. Moreover, two nonparametric statistical tests named as one sample Kolmogorov-Smirnov (KS) test and paired sample *t-test* have been carried out to identify statistical distribution as well as uniqueness of optimization algorithms. The results analysis reveals that the GWO tuned Lead-Lag based damping controller for GUPFC shows superior performance in damping low frequency oscillations for the study system.

Chapter 1

Introduction

In this chapter, an overview of the thesis has been presented that demonstrates the motivation behind this work. To the concurrent and previous technology adopted to mitigate Low Frequency Oscillation (LFO) which is the central part of this research work, has been noticeably focused in this chapter. The background of the research work has been illustrated in section 1.1. Then in section 1.2, the problem statement has been discussed. After that, in order to focus the present status of the research work relating to LFO, the research challenges have been depicted in section 1.3. Literature review is given in article 1.4. Main objective of the research work has been depicted in section 1.5. Finally, the chapter is ended with the description of thesis overview in section 1.6.

1.1 Background

Low frequency oscillation (LFO) is a prime concern for proper operation and stability of a power system, since this oscillation may result in large system excursion, leading to instability and threaten system security [1, 2]. This LFO is generated due to imbalance between mechanical input and generator active power output [3]. Based on the frequency range, LFO is classified into two categories. Inter-area mode, bounded within 0.1 to 0.8 Hz, arises due to interaction among the generators of different areas of a large power system, whereas, local mode, residing within 0.7 to 2.0 Hz, occurs as a result of interaction of a single generator with the rest of the power system [4]. To mitigate these inter-area and local modes of oscillations, rotor should provide sufficient damping torque to the system. However, failure of rotor to deliver the required damping torque makes the system unstable. Hence, integration of a controller providing additional damping torque into the system is a must for maintaining the system stability. Several research works based on different control approaches have been found to mitigate this LFO within a specified range (2-6 sec) [5, 6, 7]. Modern world with the increase in demand of energy, the difficulties of maintaining the complicated network is also increased. LFO is explicitly the active power oscillation in the power system which is a common phenomenon especially in a large network.

For years LFO has been a great concern for the researchers due to its destructive effects. LFO is also referred to as electromechanical oscillation because it associates with the change of angular position of rotors of the generators. The dynamic behavior of rotor due to small perturbation of load or source leads to breakdown of equilibrium between electromagnetic torque caused by the load and mechanical torque produced by the prime mover. The components of electromagnetic torque followed by small perturbation or disturbance is classified as synchronizing torque, which is responsible for producing aperiodic oscillation whereas another part damping torque is responsible for producing periodic oscillation. Once the LFO begins in the large power system, it may sustain for several cycles and then vanishes or grows constantly that may lead to collapse the power system. There are several sources that significantly influence on the nature of power system stability. The weak tie lines and the complicated large network structure are one of the sources for LFO. In addition to this, deficiency of available output of the plant with respect to reserve margin and significant inconsistency in the regional power are the prominent reasons of LFO.

1.2 The existing approach for the mitigation of LFO

In the last few decades, Power System Stabilizer (PSS) has been widely used to mitigate LFO and to improve stability in an effective and economical way [8]. However, inability to mitigate voltage fluctuation, introduction of leading power factor, and failure to handle severe faults (i.e. three phase faults) are few of the major shortcomings of PSS which encourage the researchers to search for new damping controllers. Fortunately, with the advancement in power electronics based fast-switching elements, application of Flexible ac Transmission System (FACTS) devices has become widespread with its excellent features of operation, controllability and transfer limits [9, 10, 11, 12, 13], which motivates the researchers to employ FACTS devices in power system domain for enhancement of the stability. Although, at the beginning, thyristor based controller such as Static VAR Compensator (SVC), Thyristor Controlled Series Compensator (TCSC), Thyristor Controlled Phase Shifter (TCPS) are widely used for mitigating LFO, due to their slow response in terms of controllability, they have been recently replaced by new generation Voltage Source Converter (VSC) based FACTS controller such as Static Synchronous Compensator (STATCOM), Static Synchronous Series Compensator (SSSC), and Unified Power Flow Controller (UPFC) [13, 10]. Among all these above mentioned FACTS devices, UPFC is widely used for single transmission used due to its

capability to enhance transient stability, to control power flow in transmission line and to mitigate LFO [14, 15]. This UPFC is limited to provide above mentioned advantages for a single transmission network. However, practical power system network generally comprises of multi-transmission line, and hence, to implement UPFC in such scenario needs some modification. This leads to the emergence of a new FACTS device named Generalized-UPFC (GUPFC), which can efficiently handle power flow, bus voltage, and LFO for more than one transmission line or even for a sub-network [16]. Hence, several research works regarding GUPFC have been done focusing on enhancement of power system stability such as mitigation of LFO and controlling of power flow [17, 18].

1.3 Research challenges

Low frequency oscillation has attracted a great deal of attention of the researchers over the years since it is considered as a significant issue for reliable operation of power system. Various controllers and optimizing techniques are being adopted to lessen the LFO for the reinforcement of the power system stability. This is why, it is focused in different literature such as-in [19], GUPFC based Single Machine Infinite Bus (SMIB) power system was presented, where a comparison of performance between GUPFC and conventional PSS was done. Again, in [20], a GUPFC based power injection model was proposed, where, it effectively controlled active and reactive power flows between two lines. However, these aforementioned works are limited with dynamic modeling of GUPFC and no detailed work regarding controlling GUPFC has been carried out. To overcome the above mentioned drawbacks of the preceding works, in [17], GUPFC and Power Oscillation Damping (POD) based control system was proposed to mitigate inter-area oscillation in multi-machine power system. However, this work contains no contribution regarding optimization of the parameters of the controller, which may lead to some sub-optimal controller gains. To address this issue, in [18], a Flower Pollination Algorithm (FPA) based optimizer was used to tune the controller parameters for GUPFC based multi-machine system.

However, none of the aforementioned works present any sort of comparative and comprehensive study among different optimization algorithms as well as different types of controllers. Furthermore, since optimization algorithms works with certain degree of probability and randomness, it is more realistic to perform statistical tests such as

quantitative and non-parametric tests to figure out statistically significant differences among different optimizers, which is also absent in the previous works.

To achieve high efficiency and high reliability of power system, many control strategies based on advanced control theories have been introduced. Model Predictive Control (MPC) is the only practical control method that takes account of system constraints explicitly, and the only 'advanced control' method to have been adopted widely in industry. To the extension of this research work, MPC will be used as the controller that usually use an online optimization in real time to determine control signals. The solution to optimization problem will be formulated with the help of the system model. At each control interval, an optimization algorithm will be attempted to determine the system dynamics by computing a sequence of control input values satisfying the control specifications.

1.4 Literature review

This section focuses on numerous methods and control strategies for the improvement of LFO from the previous and recent research works. Since the efficacy of LFO mitigation mostly depends on the effective design of damping controller, henceforth over the year's researcher's emphasis on the aspects of designing damping controller as well as the selection of the control strategy that is cited in many literatures has been included in this chapter. This section begins with the discussion of several prominent research works about GUPFC based damping controller for the improvement of LFO.

1.4.1 Research work based on GUPFC equipped system relating to LFO and power flow

A considerable number of research works have been accomplished pertaining to small signal stability to lessen the problem associated with LFO. With this aim, the research works concentrates on the improvement of damping function and the design damping controller. Linearized Phillips-Heffron model of a power system introduced with a GUPFC has been proposed in [19], where the comparative study of regular PSS and GUPFC has been presented. Although this research work presents a comprehensive model of GUPFC, this work has some limitations. Firstly, there is no specific model or design mentioned for PSS structure. Secondly, the work does not show any comparative analysis between UPFC and GUPFC that depicts superiority of GUPFC over UPFC.

Moreover, this work lacks supportive analysis in favor of the design of robust damping controller.

GUPFC based power injection model has been proposed in [20], the research work presents a power injection model comprised of GUPFC that regulates active and reactive power flow between two transmission lines .The focus of the work is to deal with small and large signal stability. Considering the most fundamental GUPFC arrangement, the structure can control four active and reactive power flow in two transmission lines. However, this aforementioned work is limited to design of power injection model of GUPFC and no detailed work regarding the parameter optimization of the POD controller incorporated with GUPFC has been performed. Development of GUPFC detailed model for the comparison with multi-UPFC has been proposed in [21]. The research work illustrates the performance analysis of multi-UPFC and GUPFC by the comparative study which deals with controlling active and reactive power flow. The model includes detailed design process of GUPFC in MATLAB-Simulink.

Optimal control method for GUPFC tuned by FPA has been proposed in [18]. In this paper FPA has been adopted to provide optimal parameters of two steps Lead-Lag controller, where the controller depicts effective performance modeled by PSS and POD. In addition to this, the research work compares the performance of numerous combination such as without FACTS system, a system with PSS, system with GUPFC, system with GUPFC and PSS, and systems with GUPFC-POD and PSS. Although this study analyzes the dynamic performance for instance rotor angle and rotor speed deviation by the comparative system response for the above mentioned case, this proposed method lacks the information regarding the robustness of the damping controller viable to all operating mode.

Modeling of GUPFC to find optimal power flow in a nonlinear interior point has been proposed in [16]. In this work, nonlinear interior point method is used to obtain the solution of optimal power flow by the development of the mathematical model of GUPFC comprised of two series converter and one shunt converter. Although the presentation and organization of the paper is excellent and it proposes an innovative method for power flow solution but the work does not deal with the concept of LFO problem.

Dynamic Simulation of GUPFC Controller for the study of Multi-Machine Power Systems has been proposed in [22]. This paper presents a novel nonlinear dynamic simulation of GUPFC comprising of one shunt converter and two series converters dependent on VSC and dc connected capacitor introduces a multi-machine control system. The linearized Phillips-Heffron model of the system has been presented with Hammons and Winning to consider the gravity of oscillation. The proposed model has been investigated in two cases, first is for two machine 12- buses and other is for 3-machines and 57- buses. The research work concentrates a great extent to damp power oscillation, but it does not include the design procedure of controller and the parameter optimization.

An LFO mitigation related work named damping of power-system oscillations with the application of a GUPFC has been presented in [23]. In this work, a control procedure has been introduced for a GUPFC with numerous controllable parameters that depend on the energy function of an entire electric-control system pondering about global parameters. The reason for the usage of such a methodology, which has been proposed in this work, is to realize the energy function of a power system that incorporates GUPFC. However, one of the crucial issues of employing energy function method is to maintain appropriate control procedure as a precondition for such technique.

1.4.2 Summary of limitations of the existing models for the improvement of LFO

From the literature review of the existing models of FACTS based damping controller, it can be inferred that there are some limitations.

- There are some research works which concentrate on the basic design of damping controller but the parameters optimization issue is ignored in those works.
- On the other hand, in some models, even though an impressive result is obtained, the contribution is limited to particular applications.
- Most of the research works related to LFO presented in this chapter used different control approach but the common limitation is that the optimization method was not examined rigorously.
- After all, this research work is being carried out for the improvement of the FACTS based models for the enhancement of LFO to get quick access, easy and reliable method indeed.

1.5 Thesis objectives

This section includes the specific objectives of this research work.

- To develop a dynamic model of an SMIB system integrated with GUPFC to study the nature of stability.
- To study the system small signal stability from the linearized model in open-loop condition and integration with controller.
- To tune the controller parameters using some meta-heuristic to find the optimal one.
- To study the dynamics of power system followed by small perturbation in time domain simulation.
- To compare the performance of the optimizers using statistical tool, time domain simulation and eigenvalue analysis to realize optimal outcome.

1.6 Thesis organization

In summary, the overview of this research work is given as follows:

- Chapter 1 illustrates background, the existing approach to mitigate LFO, literature review of existing damping controller, the methods used for the enhancement of small signal stability, research challenges and objectives with specific aims.
- Chapter 2 describes the fundamental concepts and operating principles of FACTS devices also the systematic procedure to develop dynamic model of GUPFC.
- Chapter 3 describes the details of methodology of proposed research work.
- Chapter 4 illustrates the results and discussions part of this thesis that includes eigenvalue analysis in close-loop, time domain simulation, quantitative analysis and finally, Non-Parametric statistical analysis.
- Chapter 5 is the last part of this thesis which is ended with an explanatory conclusion with future work.

Chapter 2

FACTS Devices and Mathematical Modeling of GUPFC

This chapter introduces the fundamental concepts of FACTS devices and the linearized dynamic model of GUPFC equipped SMIB system, which is the basic building block for investigating small signal stability. In the organization of this chapter, first of all, section 2.1 begins with the introduction to FACTS devices and modeling. Section 2.2 discusses the fundamental components of GUPFC. Section 2.2.1 and Section 2.2.2 describe the basic construction and function of Static Synchronous Series Compensator (SSSC) and Static Synchronous Compensator (STATCOM) respectively to realize the operating principle and control method of GUPFC. The chapter is concluded with the illustration of the operation and control strategy of the GUPFC in section 2.3. In section 2.4 of this chapter mathematical model of the GUPFC equipped SMIB system has been discussed. Finally, the chapter concludes with the illustration of the linearized model of the GUPFC equipped SMIB system in section 2.5.

2.1 Introduction to FACTS devices and modeling

Over the last several decades with the advancement of power electronics devices, application of Flexible ac transmission systems (FACTS) devices has become uncomplicated with its excellent features of operations, controllability and transfer limits [5]. At the end of the last century, to strengthen the power system the technology of FACTS controller was developed. Essentially, FACTS devices are the applications of power electronics based control that uses power electronics system along with static equipment for the manipulation of one or more parameters of high voltage ac transmission system. The numerous FACTS controller, such as thyristor controlled series capacitor (TCSC) and Static Var Compensator (SVC) is referred to as a prominent first-generation FACTS controller. Likewise, Static Synchronous Series Compensator (SSSC) and Static Synchronous Compensator (STATCOM) are the outcomes of second generation FACTS controller. Combination of series-series static synchronous series compensator (SSSC) makes Interline Power Flow Controller (IPFC) whereas a combination of series-shunt (SSSC- STATCOM) FACTS devices forms Unified Power Flow Controller (UPFC). Generalized Unified Power Flow Controller (GUPFC) is another third

generation FACTS device named as multiline UPFC treated as the most leading-edge FACTS controller and offers better control abilities contrasted with other controllers. Although the FACTS controllers are as yet considered costly contrasted with the ordinary power system controllers, they have been introduced in numerous real power system on the world because of their prevalent control execution capability [24]. Indeed, in order to regulate line power flow and to improve voltage profile, mechanically controlled series and shunt capacitors were used since the beginning of FACTS devices as early as the 1920s when the operating principle of FACTS controller is known. The application of power electronics devices was prevalent when mercury valve was replaced by thyristor in controlling high voltage dc systems. The new age of FACTS controllers utilizes self-commutated voltage source based power converters to realize quickly controllable, static synchronous ac voltage or current sources. Another age FACTS controller is built essentially on the Synchronous Voltage Source (SVS) which is a perfect machine with no rotation and inertia.

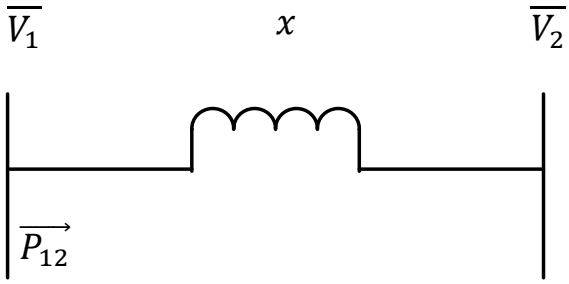

Figure 2.1: Circuit diagram for the illustration of the operational principle of FACTS controllers

The magnitude and phase of the SVS can be controlled instantly to create reactive power (both capacitive and inductive) as well as to regulate active power flow that is not influenced by the variables affecting power flow (voltage and current) [3].The fundamental principle of the FACTS controllers can be illustrated by the Fig. 2.1 [25]. The real power transferred along the transmission line is expressed as following:

$$\overrightarrow{P_{12}}=\frac{\overrightarrow{V_1}\ \overrightarrow{V_2}}{x}\sin\theta \qquad 2.1$$

Where θ is the phase angle difference between the voltage at the sending end, $\overrightarrow{V_1}$ and receiving end of the transmission line, $\overrightarrow{V_2}$ In order to control power flow along the transmission line it is indispensable for a FACTS controller to change the line impedance *x*

with time, the magnitude of line voltage ($\overrightarrow{V_1}$,$\overrightarrow{V_2}$), and phase angle separately to such an extent that superior adaptability of power flow management is accomplished [26, 27].

2.2 Fundamental components of GUPFC

To understand the comprehensive model of GUPFC, it is essential to realize the basic component of GUPFC. As stated earlier, SSSC and STATCOM are the core element of GUPFC that use VSC based converter and there is some dissimilarities from first generation thyristor based FACTS device. The basic block diagram and function of these elements are shown in Fig. 2.2.

2.2.1 Static Synchronous Series Compensator (SSSC)

Static Synchronous Series Compensator (SSSC) is a modern power quality FACTS device that employs a voltage source converter connected in series to a transmission line through a transformer. The SSSC operates like a controllable series capacitor and series inductor. The primary difference is that its injected voltage is not related to the line intensity and can be managed independently. This feature allows the SSSC to work satisfactorily with high loads as well as with lower loads. SSSC has three basic components:

a) Voltage Source Converter (VSC) – main component
b) Transformer – couples the SSSC to the transmission line
c) Energy Source – provides voltage across the DC capacitor and compensation

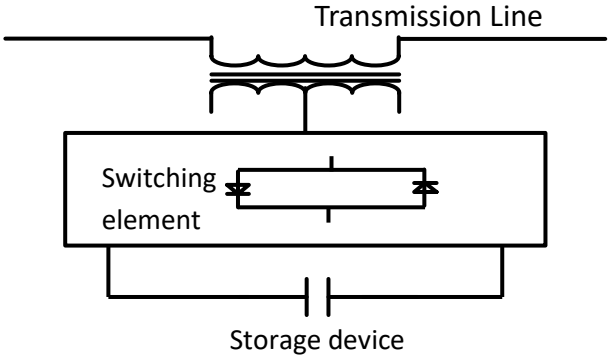

Figure 2.2: Schematic diagram of SSSC

SSSC having storage source can alternate the flow of real power with the power system. With an appropriate control arrangement, the can SSSC be utilized to control the transmission of power. As the reactive compensator, the SSSC has two magnitude nodes a) the constant reactance mode and b) the constant Quadrature voltage mode. In the first case, the SSSC

voltage has a dependency on the line current while in the latter case it is independent of line current [28, 29, 30].

2.2.2 Static Synchronous Compensator (STATCOM)

Static Synchronous Compensator (STATCOM) is a shunt-connected FACTS device. It is like the static counterpart of the rotating synchronous condenser, but it generates or absorbs reactive power at faster rate because no moving parts are involved. It is operated as a SVC whose capacitive or inductive output currents are regulated to control the bus voltage with which it is connected. In principle, it performs the same voltage regulation as the SVC but in a more robust manner because unlike the SVC, its operation is not impaired by the presence of low voltages. It goes on well with advanced energy storage facilities, which opens the door for a number of new applications, such as energy deregulations and network security. STATCOM operation is based on the principle of voltage source or current source converter [31]. The schematic of a STATCOM is shown in Fig. 2.3 when used with VSC, its ac output voltage is controlled such that the required reactive power flow can be controlled at the generator or load bus with which it is connected.

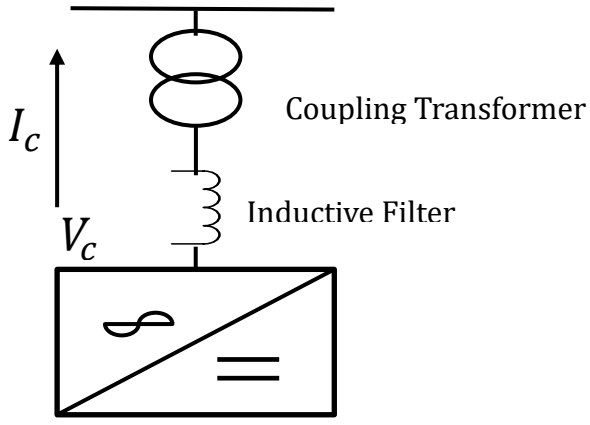

Figure 2.3: Schematic diagram of STATCOM

Due to the presence of dc voltage source in the capacitor, the VSC converts its voltage to ac voltage source and controls the bus voltage [32, 33].

2.3 Operation and control strategy of GUPFC

In order to keep up the voltages profile in the electrical network of power system within the satisfactory limit nowadays the use of FACTS controller are versatile, among them GUPFC is one of the prominent FACTS devices which manipulate VSC in order to inject adjustable voltages in series with the transmission line. Each injected voltage can have a positive or negative magnitude with a phase angle varying from $-\pi/2$ to $\pi/2$. These sources have the capability to contribute a voltage at any angle pertaining to the line current. By injecting or absorbing the voltages into the transmission line it performs the tasks of exchanging real and reactive power between the transmission lines. In this research work, two transmission line structures are considered. The GUPFC is comprised of three VSC based converters of the kind of one shunt and two series which are connected to the transmission line via exciting and boosting transformer respectively. The real and reactive power demanded by the boosting VSC is provided by the excitation VSC. There is a dc link capacitor between the shunt and series converter which permits the bi-directional real power flow in order to minimize the imbalance caused by the perturbation or disturbance in the transmission line. The structure used in the research work essentially acts as an ac-ac converter which is comprised of both dc and ac terminal.

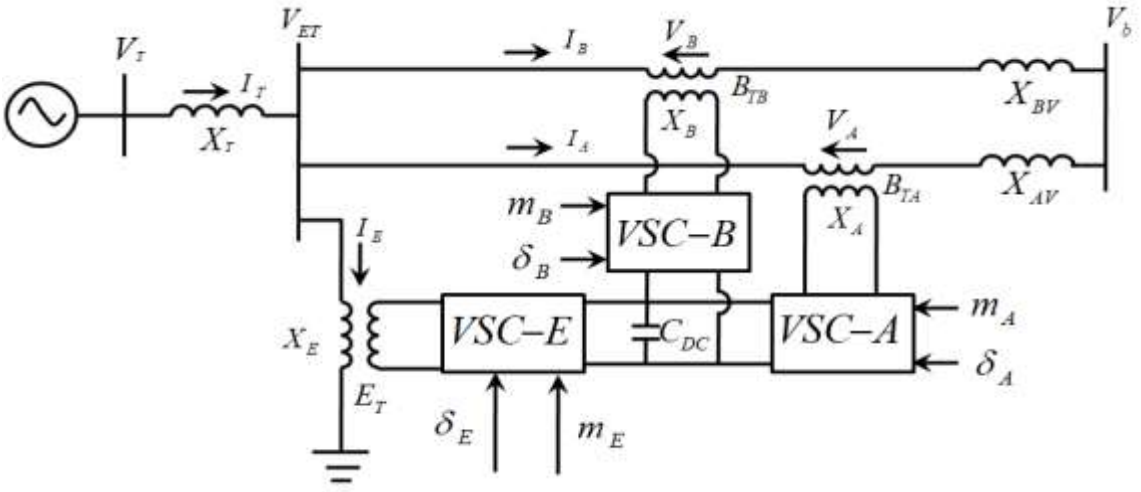

Figure 2.4: Schematic model of GUPFC-integrated SMIB system

The function of ac terminals of both shunt and series converter is to permit real power flow in either direction, also ac terminal output of each of the converter regulates the tasks of injecting or absorbing reactive power in the transmission line which is generated by VSC

converter itself. There are six controllable signals which work as an input to the GUPFC. Injection or absorption of shunt branch voltage is regulated by excitation phase angle and amplitude modulation ratio δ_E, m_E whereas series branch voltage is regulated by m_A, δ_A, m_B, δ_B referred to as boosting phase angle and amplitude modulation ratio respectively. In the GUPFC, control of real and reactive power flow is essentially maintained by VSC using the regulation of controllable signals magnitude and phase angle. In addition to this, injected voltage to the transmission line provided by the converter acts as an ac voltage source and when the line current flows through the VSC converter consequently real and reactive power is maintained in between transmission line and VSC. Current through (I_A) the line when a GUPFC is introduced is depicted in Fig. 2.4.

For Series branch

Using Kirchhoff's Voltage Law to the circuit delineated in Fig. 2.4, the following equations are obtained

$$V_{ET}\angle\delta_{ET} \pm V_B\angle\Psi_b - V_b\angle\delta_r - I_B\angle\lambda_b(jX_{BV}) = 0 \quad (2.2)$$

Solving for line current, the following equation is obtained.

$$I_B\angle\lambda_b = \frac{V_{ET}\angle\delta_{ET} \pm V_B\angle\Psi_b - V_b\angle\delta_r}{(jX_{BV})} \quad (2.3)$$

Here, V_{ET} and δ_{ET} denotes the magnitude of sending end voltage and corresponding phase angle respectively. V_b and δ_r denotes the magnitude of receiving end voltage and corresponding phase angle respectively. V_B and Ψ_b denotes the magnitude of injected voltage and corresponding phase angle respectively. X_{BV} represents reactance of transmission line. It is to be noted that, in this research work the lossless transmission line is considered. It is obvious from the equation (2.3) that by regulating the magnitude and phase angle of the injected voltage which is mainly controlled by six controllable input signals of the GUPFC we can achieve desired voltage profile and power flow of the transmission line.

2.4 Mathematical model of GUPFC equipped SMIB system

In this work, to represent GUPFC equipped SMIB system, a third order flux decay model of a synchronous generator has been considered to describe electromechanical swing equation and q-axis transient voltage dynamics, and IEEE-ST1 model to express excitation system of SMIB [31]. It is to be noted that the above mentioned third order dynamic model of generator and excitation system accurately represents the influence of steady-state and dynamic d-q

axis reactances on overall system performance whenever the mitigation of LFO in power system is of primary concern [4, 32]. Additionally, consideration of dynamic field excitation allows the viability of establishing control in generator terminal voltage. Hence, the dynamic model of the generator and excitation system considered for this work is expressed as follows.

$$\dot{\delta} = \omega_0(\omega - 1) \tag{2.4}$$

$$\dot{\omega} = \frac{1}{M}[P_m - P_e - D\Delta\omega] \tag{2.5}$$

$$\dot{E_q}' = \frac{1}{T'_{d0}}[-E_q + E_{fd}] \tag{2.6}$$

$$\Delta\dot{E}_{fd} = \frac{1}{T_A}[K_A(V_{t0} - V_t) - \Delta E_{fd}] \tag{2.7}$$

Equation (2.4-2.7) represents the dynamic state equation of the third order generator model [33]. Where,

$$P_e = V_{Td}I_{Td} + V_{Tq}I_{Tq}$$

$$E_q = E'_q + (X_d - X'_d)I_{Td}$$

$$V_{Tq} = E'_q - X'_d I_{Td}$$

$$V_{Td} = X_q I_{Tq}$$

$$V_T = \sqrt{V_{Td}^2 + V_{Tq}^2}$$

$$I_{Tq} = I_{Eq} + I_{Aq} + I_{Bq}$$

$$I_{Td} = I_{Ed} + I_{Ad} + I_{Bd}$$

Now, as GUPFC has been incorporated into SMIB system, the dc-link voltage dynamics of GUPFC is obtained using KCL illustrated in Fig 2.4, which can be presented by following equation [14].

$$\dot{V}_{dc} = \frac{m_E}{2C_{dc}} \times [I_{Ed}cos\delta_E + I_{Eq}sin\delta_E] + \frac{m_A}{2C_{dc}} \times \left[I_{Ad}cos\delta_A + I_{Aq}sin\delta_A\right] + \frac{m_B}{2C_{dc}} \times [I_{Bd}cos\delta_B + I_{Bq}sin\delta_B] \tag{2.8}$$

Again, the non-linear equations of the GUPFC are associated with the branch currents (I_A, I_B, I_E), since VSCs are coupled with transmission lines and these branch currents are required to calculate generator output power (P_e). Hence, calculation of the branch currents of transmission lines is needed. This calculation is performed using terminal and excitation bus voltage equation derived from the network illustrated in Fig. 2.4 and voltage equations of excitation and boosting transformers. The terminal and excitation voltage are expressed as follows [34].

$$V_T = jX_T I_{Td} + V_{ET} \tag{2.9}$$

$$V_{ET} = V_{AT} + jX_{AV} I_A + V_b \tag{2.10}$$

$$V_{ET} = V_{BT} + jX_{BV} I_B + V_b \tag{2.11}$$

Now, from three phase dynamics equations of GUPFC system, after neglecting transformer's resistance and transient and then applying Park's transformation, d- q axis non-linear voltage equations of excitation and boosting transformers is obtained, which are as follows [35].

$$\begin{bmatrix} V_{ETd} \\ V_{ETq} \end{bmatrix} = \begin{bmatrix} 0 & -X_E \\ X_E & 0 \end{bmatrix} \begin{bmatrix} I_{Ed} \\ I_{Eq} \end{bmatrix} + \begin{bmatrix} \frac{m_E cos\delta_E V_{dc}}{2} \\ \frac{m_E sin\delta_E V_{dc}}{2} \end{bmatrix} \tag{2.12}$$

$$\begin{bmatrix} V_{ATd} \\ V_{ATq} \end{bmatrix} = \begin{bmatrix} 0 & -X_A \\ X_A & 0 \end{bmatrix} \begin{bmatrix} I_{Ad} \\ I_{Aq} \end{bmatrix} + \begin{bmatrix} \frac{m_A cos\delta_A V_{dc}}{2} \\ \frac{m_A sin\delta_A V_{dc}}{2} \end{bmatrix} \tag{2.13}$$

$$\begin{bmatrix} V_{BTd} \\ V_{BTq} \end{bmatrix} = \begin{bmatrix} 0 & -X_B \\ X_B & 0 \end{bmatrix} \begin{bmatrix} I_{Bd} \\ I_{Bq} \end{bmatrix} + \begin{bmatrix} \frac{m_B cos\delta_B V_{dc}}{2} \\ \frac{m_B sin\delta_B V_{dc}}{2} \end{bmatrix} \tag{2.14}$$

Then, using equation 2.9-2.11 and rearranging the d-q axis components of branch current, the following equations are obtained.

$$I_{Aq} = \frac{1}{X_{q\Sigma}} [X_6 V_b \sin\delta + V_{dc}(-0.5X_{BB}X_{qE}m_E \cos\delta_E + 0.5X_2 m_A \cos\delta_A - X_E X_{qE} m_B \cos\delta_B)] \tag{2.15}$$

$$I_{Ad} = \frac{1}{X_{d\Sigma}}[-X_7 V_b \cos\delta + V_{dc}(0.5X_{BB}X_{dE}m_E \sin\delta_E - 0.5X_4 m_A \sin\delta_A + X_E X_{dE} m_B \sin\delta_B) + 2X_{BB}X_E E_{qp}] \quad (2.16)$$

$$I_{Bq} = \frac{1}{X_{q\Sigma}}[X_9 V_b \sin\delta + V_{dc}(-0.5X_{AA}X_{qE}m_E \cos\delta_E + 0.5X_{11} m_B \cos\delta_B - X_E X_{qE} m_A \cos\delta_A)] \quad (2.17)$$

$$I_{Bd} = \frac{1}{X_{d\Sigma}}[-X_{10} V_b \cos\delta + V_{dc}(0.5X_{AA}X_{dE}m_E \sin\delta_E - 0.5X_{12} m_B \sin\delta_B + X_E X_{dE} m_A \sin\delta_A) + 2X_{AA}X_E E_{qp}] \quad (2.18)$$

$$I_{Eq} = \frac{1}{X_{q\Sigma}}[X_8 V_b \cos\delta + V_{dc}(0.5X_{BB}X_{dE}m_E \sin\delta_A + 0.5X_3 m_E \sin\delta_E + 0.5\, X_{AA}X_{dE} m_B \sin\delta_B) + X_{AA}X_{BB}E_{qp}] \quad (2.19)$$

$$I_{Ed} = \frac{1}{X_{d\Sigma}}[-X_5 V_b \sin\delta + V_{dc}(-0.5X_{AA}X_{qE}m_B \cos\delta_B + 0.5X_1 m_E \cos\delta_E + X_{BB}X_{dE} m_A \cos\delta_A)] \quad (2.20)$$

Where,

$$X_{q\Sigma} = 2X_{AA}X_{BB}X_E + X_{AA}X_{BB}X_{qE} + 2X_{AA}X_E X_{qE} + 2X_{BB}X_E X_{qE}$$

$$X_{d\Sigma} = 2X_{AA}X_{BB}X_E + X_{AA}X_{BB}X_{dE} + 2X_{AA}X_E X_{dE} + 2X_{BB}X_E X_{dE}$$

$$X_{AA} = X_A + X_{AV}\,; \qquad X_{BB} = X_B + X_{BV}$$

$$X_{dE} = X_{dp} + X_{tE}\,; \qquad X_{qE} = X_{qp} + X_{tE}$$

$$X_1 = X_{BB}X_{qE} + X_{AA}X_{qE} + X_{AA}X_{BB}$$

$$X_2 = 2X_{BB}X_E + X_{BB}X_{qE} + 2X_E X_{qE}$$

$$X_3 = X_{BB}X_{dE} + X_{AA}X_{dE} + X_{AA}X_{BB}$$

$$X_4 = 2X_{BB}X_E + X_{BB}X_{dE} + 2X_E X_{dE}$$

$$X_5 = X_{BB}X_{qE} + X_{AA}X_{qE}$$

$$X_6 = 2X_{BB}X_E + X_{BB}X_{qE}$$

$$X_7 = 2X_{BB}X_E + X_{BB}X_{dE}$$

$$X_8 = X_{BB}X_{dE} + X_{AA}X_{dE}$$

$$X_9 = X_{AA}X_{qE} + 2X_{AA}X_E$$

$$X_{10} = X_{AA}X_{dE} + 2X_{AA}X_E$$

$$X_{11} = 2X_{AA}X_E + X_{AA}X_{qE} + 2X_EX_{qE}$$

$$X_{12} = 2X_{AA}X_E + X_{AA}X_{dE} + 2X_EX_{dE}$$

Here, combined reactances of the study system have been represented by the symbol X_1 through X_{12}. In the next section, the linearized system matrix will be formulated from this non-linear mathematical model of GUPFC equipped SMIB system to carry out eigenvalue and participation factor analysis for open-loop condition [36, 37, 38].

2.5 Linearized model of GUPFC equipped SMIB system

Here, in this section, linearization algorithm has been employed to above mentioned non-linear mathematical model to develop the linearized form for each corresponding dynamic equations (i.e. Eq. 2.1-2.5), since this linearized form is well suited for study of small signal stability [3]. With this aim, Taylor-series expansion has been applied to these dynamic equations and truncate higher order terms in order to obtain corresponding linearized equations. It is to be noted that, truncation of higher order term will sacrifice some accuracy, since nonlinearities associated with higher order terms are being ignored [39]. However, as aforementioned, since small perturbation is considered for this work, the linearized representation of system dynamic equations is considered significantly accurate [40]. Now, after resorting to Taylor series expansion and considering first order dynamic system equations (Eq. 2.1-2.5), the following linearized equations is obtained:

$$\Delta\dot{\delta} = \omega_0\Delta\omega \tag{2.21}$$

$$\Delta\dot{\omega} = \frac{1}{M}(-\Delta P_e - D\Delta\omega) \tag{2.22}$$

$$\Delta\dot{E}'_q = \frac{1}{T'_{d0}}(-\Delta E_q + \Delta E_{fd}) \tag{2.23}$$

$$\Delta\dot{E}_{fd} = \frac{-1}{T_A}[K_A\Delta V_t + \Delta E_{fd}] \tag{2.24}$$

$$\Delta\dot{V}_{dc} = K_7\Delta\delta + K_8\Delta E'_q - K_9\Delta V_{dc} + K_{ce}\Delta m_E + K_{c\delta e}\Delta\delta_E + K_{ca}\Delta m_A + K_{c\delta a}\Delta\delta_A + K_{cb}\Delta m_B + K_{c\delta b}\Delta\delta_B \tag{2.25}$$

Equations (2.21 -2.25) are the linearized form of system dynamic states.

Where,

$$\Delta P_e = K_1\Delta\delta + K_2\Delta E'_q + K_{pd}\Delta V_{dc} + K_{Pe}\Delta m_E + K_{P\delta e}\Delta\delta_E + K_{Pa}\Delta m_A + K_{P\delta a}\Delta\delta_A + K_{Pb}\Delta m_B + K_{P\delta b}\Delta\delta_B$$

$$\Delta E_q = K_4\Delta\delta + K_3\Delta E'_q + K_{qd}\Delta V_{dc} + K_{qe}\Delta m_E + K_{q\delta e}\Delta\delta_E + K_{qa}\Delta m_A + K_{q\delta a}\Delta\delta_A + K_{qb}\Delta m_B + K_{q\delta b}\Delta\delta_B$$

$$\Delta V_t = k_5\Delta\delta + K_6\Delta E'_q + K_{vd}\Delta V_{dc} + K_{ve}\Delta m_E + K_{v\delta e}\Delta\delta_E + K_{va}\Delta m_A + K_{v\delta a}\Delta\delta_A + K_{vb}\Delta m_B + K_{v\delta b}\Delta\delta_B$$

Here, k_1-k_9 are termed as linearization constant. Now, it is well-known from the literature that, the linearized form allows us to represent the system using standard state space model of the form: $\dot{\Delta x} = A\Delta x + B\Delta u$, where state vector $x = [\Delta\delta \quad \Delta\omega \quad \Delta E'_q \quad \Delta E_{fd} \quad \Delta V_{dc}]$, control vector $u = [\Delta m_e \quad \Delta\delta_E \quad \Delta m_A \quad \Delta\delta_A \quad \Delta m_B \quad \Delta\delta_B]^T$, and A and B are commonly termed as system matrix and input matrix. The matrix A and B eventually helps to calculate the system eigenvalues, participation factor, and controllability index under open-loop condition [41]. Hence, in this work, exploiting DAE of Eq. 2.21-2.25 and eliminating the algebraic linearized variables (i.e. ΔP_e , ΔE_q , ΔV_t), system matrix A and input matrix B are obtained as follows.

$$A = \begin{bmatrix} 0 & \omega_b & 0 & 0 & 0 \\ -\frac{K_1}{M} & -\frac{D}{M} & -\frac{K_2}{M} & 0 & -\frac{K_{pd}}{M} \\ -\frac{K_4}{T'_{d0}} & 0 & -\frac{K_3}{T'_{d0}} & \frac{1}{T'_{d0}} & -\frac{Kqd}{T'_{d0}} \\ -\frac{K_A K_5}{T_A} & 0 & -\frac{K_A K_6}{T_A} & -\frac{1}{T_A} & -\frac{K_A K_{vd}}{T_A} \\ K_7 & 0 & K_8 & 0 & -K_9 \end{bmatrix}$$

$$B = \begin{bmatrix} 0 & 0 & 0 & 0 & 0 & 0 \\ -\frac{K_{pe}}{M} & -\frac{K_{p\delta e}}{M} & -\frac{K_{pa}}{M} & -\frac{K_{p\delta a}}{M} & -\frac{K_{pb}}{M} & -\frac{K_{p\delta b}}{M} \\ -\frac{K_{qe}}{T'_{d0}} & -\frac{K_{q\delta e}}{T'_{d0}} & -\frac{K_{qa}}{T'_{d0}} & -\frac{K_{q\delta a}}{T'_{d0}} & -\frac{K_{qb}}{T'_{d0}} & -\frac{K_{q\delta b}}{T'_{d0}} \\ gK_{pe} & gK_{p\delta e} & gK_{pa} & gK_{p\delta a} & gK_{pb} & gK_{p\delta b} \\ K_{ce} & K_{c\delta e} & K_{ca} & K_{c\delta a} & K_{cb} & K_{c\delta b} \end{bmatrix}$$

Where, $g = \frac{K_A}{T_A}$

The above mentioned system matrix A and input Matrix B is used to describe the property of the system. From the stability theory, it is experienced that if anyone of the eigenvalues of the system matrix lies in the right of half-s plane the system is said to be unstable. A and B are the constant matrices with appropriate dimensions which are dependent on the operating point of the system. The eigenvalues of the state matrix A that are called the system modes define the stability of the system when it is affected by a small perturbation. As long as all eigenvalues have negative real parts, the power system is stable when it is subjected to a small disturbance. If one of these modes has a positive real part the system is unstable. In general, state equation shows the relationship between the system's current state with its input, and the future state of the system. The output equation shows the relationship between the system state with its input and the output. These equations show that in a given system, the current output is dependent on the current input and the current state. The future state is also dependent on the current state and the current input.

Chapter 3

Methodology

In this chapter basic procedure has been discussed that are used to investigate LFO, generated in the large and complicated electrical networks due to various perturbations. The fundamental steps that have been followed in this work to deal with small signal stability problems are, to examine unstable mode from the open loop analysis and identification of the most suitable control signal by determining controllability index and residue index. In the organization of this chapter, section 3.1 discusses the procedure of determining equilibrium point and linearization approach. Open loop eigenvalue analysis method is illustrated in section 3.2. With the flow of discussion, section 3.2.1 and 3.2.2 describes eigenvector calculation and the formation of participation factor matrix respectively. Identification of unstable mode from the open-loop analysis has been illustrated in the sub section 3.2.3. One of the significant parts for designing effective damping controller is to choose suitable control signal. Hence, approach for identification of the most appropriate control signal has been discussed in section 3.3. The design of the damping controller and optimization procedure has been included in section 3.4. The design procedure of the close-loop system is discussed in section 3.5. In section 3.6, illustration of optimization algorithm has been incorporated. Section 3.7 describes the objective functions used in this work. One of the central parts of this research work in included in section 3.8 which discusses controller parameter optimization procedure. At the end, the chapter concludes with the discussion of time domain analysis.

3.1 Determination of equilibrium point and linearization approach

The general mathematical model of a power system that is used to investigate LFO can be represented by the following equation. Considering a general nonlinear model with n state variables, m input variables, and r output variables the vector notation of the equation takes the following form

$$\dot{x} = f(x_n, u_m) \tag{3.1}$$

$$y = g(x_n, u_m) \tag{3.2}$$

Where the state vector can be represented as following

$$\begin{aligned} \dot{x}_1 &= f_1(x_1, \dots x_m, u_1, \dots u_m) \\ &\vdots \\ \dot{x}_n &= f_n(x_1, \dots x_m, u_1, \dots u_m) \end{aligned}$$

$$\dot{y}_1 = g_1(x_1, \dots x_m, u_1, \dots u_m)$$
$$\vdots$$
$$\dot{y}_n = g_r(x_1, \dots x_m, u_1, \dots u_m)$$

$$A_{ij} = \left.\frac{\partial f_i}{\partial x_j}\right|_{x_s, u_s,} \qquad C_{ij} = \left.\frac{\partial g_i}{\partial x_j}\right|_{x_s, u_s,}$$

$$B_{ij} = \left.\frac{\partial f_i}{\partial u_j}\right|_{x_s, u_s,} \qquad D_{ij} = \left.\frac{\partial g_i}{\partial u_j}\right|_{x_s, u_s,}$$

From equation 3.1 and 3.2, state vector $\dot{x}$ and output matrix y are represented by the function f and g respectively. Both of the functions are dependent on state matrix with n×n dimension and input matrix with m×n dimension. In this research work the state of the system n is 5 and input m is 6. In general the state space equation can be represented as follows

$$\dot{X} = Ax + Bu$$
$$y = Cx + Du$$

The above mentioned system matrix A and input Matrix B can be used to describe the property of the system. From the stability theory, it is experienced that if anyone of the eigenvalues of the system matrix lies in the right of half-s plane the system is said to be unstable. A and B are the constant matrices with appropriate dimensions which are dependent on the operating point of the system. The eigenvalues of the state matrix A that are called the system modes define the stability of the system when it is affected by a small interruption.

3.2 Open loop eigenvalue analysis

One of the common and effective methods to investigate small signal stability is eigenvalue analysis of the system matrix at an operating condition. By inspecting the nature or mode of eigenvalue the characteristic of the oscillation can be identified. Furthermore the participation factors which is derived from the left and right eigenvectors corresponding to the eigenvalues of the system matrix indicates the contribution of the eigenvalue of the system matrix in producing LFO. Again oscillation frequency and damping ratio calculated from the eigenvalue can help designing and finding the effectiveness of damping controller. The information

regarding the dominant state of the system matrix calculated by participation matrix gives clear conception of the oscillatory mode.

The basic steps that are followed in this research work to investigate the LFO have been shown in Fig. 3.1

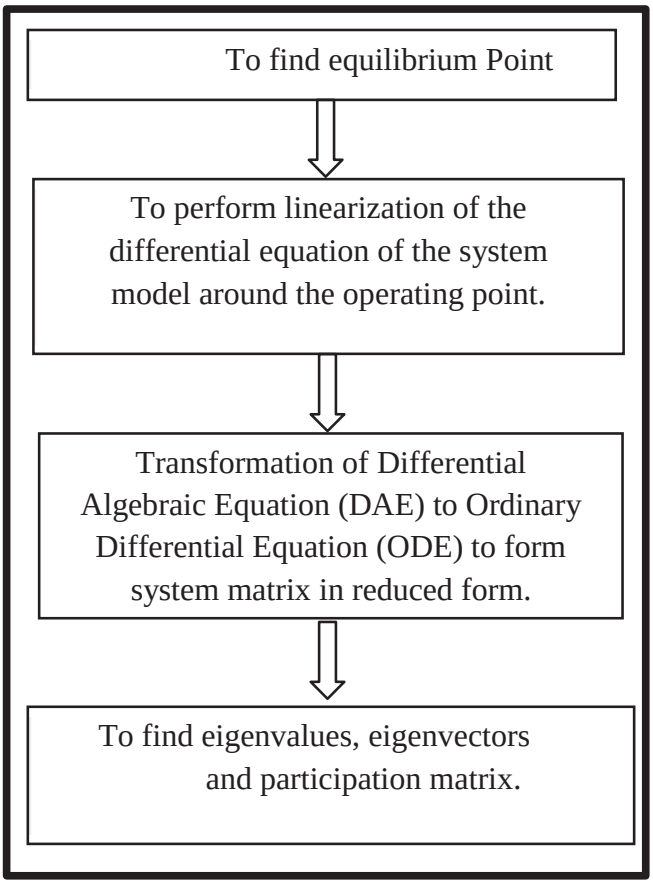

Figure 3.1: Fundamental steps of LFO study through eigenvalue analysis

3.2.1 Determination of eigenvalues, eigenvectors and participation matrix

By observing the reduced system state matrix it is easy to inspect the nature of steady state stability or small signal stability around the operating point. It is to be mentioned that the number of state and eigenvalue rely on the dimension of reduced system matrix.

$$[A - \lambda I]\phi = 0 \tag{3.3}$$

Where λ represents eigenvalue and ϕ represents right eigenvector. For non-trivial solution determinant of $[A - \lambda I]$ equals to zeros and the eigenvalues can be calculated. Similarly, another equation can be written to find out the left eigenvector ϕ as given in (3.3)

$$[A - \lambda I]\psi = 0 \tag{3.4}$$

The right eigenvector provides the information (equation 3.4) how each of the system state is influenced by the oscillatory mode. Alternately, it determines the modal observability of the system hence another name of right eigenvector is mode shape. Conversely the information regarding amplitude of the mode is obtained from system's initial state and left eigenvector. In addition to this, information related to controllability is also obtained by left eigenvector. Eigen vector is an useful tool to find mode sensitivity, transfer function residues and participation factors. Planning of Controller design and for the analysis of system states, mode sensitivity, transfer function residues and participation factor plays vital role. It is to be mentioned that all the eigenvalues of the system matrix should lie in the left half plane to make the system stable. This implies the position of the real part of complex conjugate must be placed in the left half plane. It is noticed explicitly that in the event of unstable mode real part always lies in the right half plane even it is complex conjugate [44]. From the eigenvalue in complex format,$-\alpha \pm j\beta$, damping ratio (ζ) and the natural frequency of oscillation (f) can be calculated using equation (3.5) and equation (3.6) respectively.

$$\zeta = \frac{-\alpha}{\sqrt{(\alpha^2 + \beta^2)}} \tag{3.5}$$

$$f = \frac{\beta}{2\pi} \tag{3.6}$$

3.2.2 Formation of participation factor matrix

Once both right and left eigenvectors are known for different eigenvalues, the participation factor matrix can be calculated by combining the left and right eigenvectors as shown in equation (3.7)

$$P = [P_1, P_2, \ldots . P_n] \tag{3.7}$$

$$\text{With } P_i = \begin{bmatrix} P_1 \\ P_2 \\ \ldots . \\ P_n \end{bmatrix} = \begin{bmatrix} \emptyset_{1i}\psi_{i1} \\ \emptyset_{2i}\psi_{i2} \\ \ldots . \\ \emptyset_{ni}\psi_{in} \end{bmatrix}$$

Where right eigenvector and left eigenvector of the i_{th} mode are expressed as Φ_{ki} and ψ_{ik} respectively [43].

3.2.3 Identification of unstable mode from open- loop analysis

The state equations obtained from the linearized model is used to find eigenvalues of the system matrix that provide information regarding stability of the system. There is an electromechanical oscillation mode associated with machine inertia found in the eigenvalue analysis. To choose the most effective stabilizer for the control of oscillation, identification of the electromechanical oscillation mode related to eigenvalue is required. It is observed that dominant oscillation mode accountable for the electromechanical oscillation is closely linked to the rotor motion equation of generators and can be identified by investigating the complex conjugate eigenvalue having higher participation factors than those of other state variables [3]. In this research work, participation factors method is used and that will be discussed in the subsequent section [45].

3.3 Identification of the most effective control signal

Before integrating controller into the study system, identification of the best control signal is needed from available six signals (i.e. m_E , δ_E, m_A , δ_A , m_B, δ_B) of GUPFC, since the best one has the greatest impact on enhancing the damping of unstable EM mode of oscillation (i.e. $\Delta\delta$, $\Delta\omega$) for the system [46]. To understand the substance regarding the controller design for choosing the most effective control signal controllability index, observability index and residue analysis are commonly used. In order to design a controller these two significant properties named controllability index and observability index are well studied to find desired outcome. It is to be noted that the features of the controllability is to handle the control input for adjusting the system state to a desired one. Besides this, uncontrollable state cannot be controlled by control input. Again property of observability helps finding the initial state whether it is observable from the output or not. It is not possible to determine the particular state behavior from the system output unless it is observable hence not suited to stabilize that state. Controlabilty index, observability index and residue are calculated from eigenvector corresponding to the oscillatory mode.

With this aim, controllability and residue index have been calculated using following equations for each of these signals [47, 48].

$$r_{ki} = b_{ki} O_i \tag{3.8}$$

$$b_{ki} = W_i^T B_k \tag{3.9}$$

Here, *i* correspond to the i_{th} state of eigenvalue, which in this case are 4 and 5, since they are associated with EM mode as illustrated in Table 3.2. Moreover, $k = 1 \ldots 6$, which is the

column number of input matrix B, O_i is the observability index for the corresponding EM modes. W_i^T is the left eigenvalue for EM modes of the system matrix A, B is the input matrix presented in linearization section. The result obtained from controllability and residue index calculation is presented in Table. 3.1

Table 3.1: Comparison of controllability and residue index among six control signals of GUPFC

Control signal	Controllability index	Residue index
m_E	0.3471	0.1582
δ_E	3.9325	1.3975
m_A	3.9186	1.3720
δ_A	0.9571	0.3351
m_B	3.9186	1.3720
δ_B	0.9571	0.3351

This figure depicts that δ_E control signal has significant impact on the improvement of the negatively damped EM mode than other control signals of GUPFC, since δ_E shows higher magnitude (3.9123, 1.3975) in both controllability and residue index respectively. Hence, δ_E has been considered as the most appropriate control signal for controller design. Again to figure out the stability nature, open-loop condition has been examined that is presented in Table 3.2

Table 3.2: Eigenvalues and participation factor analysis for study system in open-loop condition

Eigenvalue	Associated state	Participation factor
−85.2473	ΔE_{fd}	85.48
−15.3535	ΔE_q	84.67
−0.0685	ΔV_{dc}	99.89
0.0682±6.0230i	$\Delta\delta$, $\Delta\omega$	49.31, 49.31

From the Table 3.2, it is observed that the unstable state is associated with the EM mode and the corresponding damping ratio is -0.0019 with an oscillation frequency of 0.9585 Hz.

3.4 Design of damping controller and optimization procedure

In the power system stability studies, a damping controller is used to reduce the system oscillation when any disturbance occurs. The online tuning of these controller's parameters is always a challenge to the power engineers and by applying any adaptive soft-computing technique [2].

In case of small signal stability when the system is subjected to sudden change consequently perturbation occurs around the equilibrium point that results in power oscillation. Unless adequate damping is provided to damp this power oscillation, it leads to systems failure. In order to resolve power oscillation damping different supplemental control is used in corporation with FACTS devices.

In this work, two different controllers named PI and Lead-Lag is adopted as supplementary controller applied to GUPFC which is denoted as Power Oscillation Damping (POD). To mitigate LFO, it is needed to increase system damping by diminishing electromechanical oscillations hence POD control action is adopted in this proposed method in concern with GUPFC. It is customary to place GUPFC in the transmission line to regulate active or reactive power flow along the line and generally speed deviation ($\Delta\omega$) is preferred as the input to the PI or Lead-Lag controller of GUPFC [6].

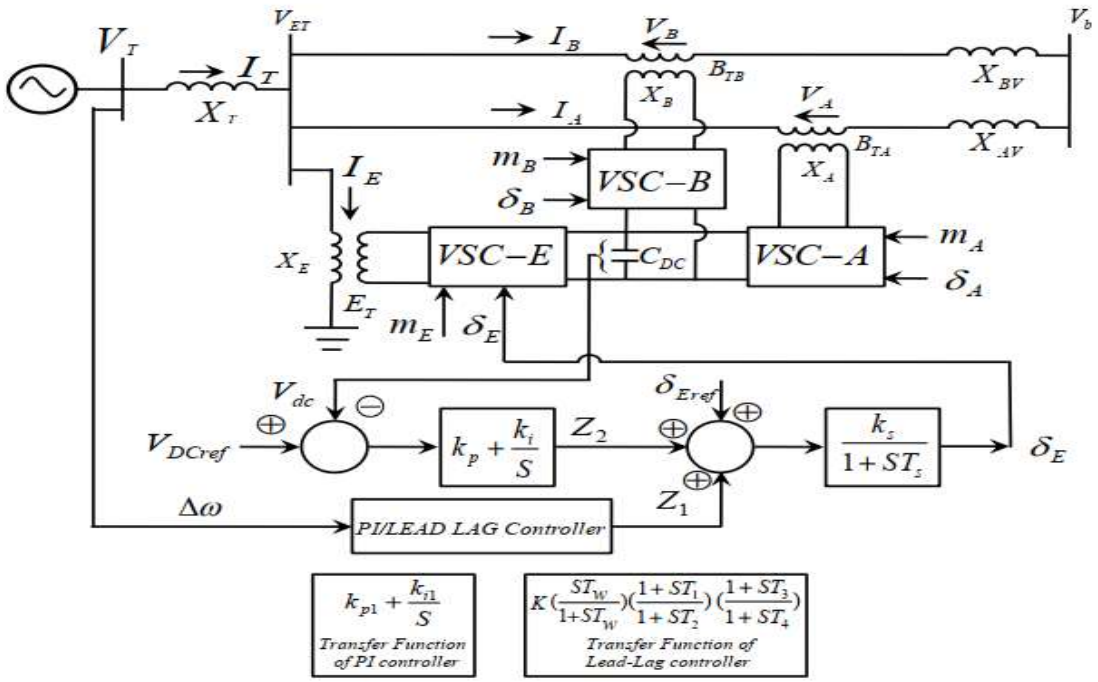

Figure 3.2: Close loop configuration of GUPFC-integrated SMIB system

3.5 Close-loop system formulation

Here, in order to formulate close-loop system, two widely adopted controllers such as PI and lead-lag controllers are included to obtain the most effective control signal δ_E found in the previous sub-section in order to improve damping ratio for negatively damped unstable EM mode. The close-loop system of the study system is shown in figure in Fig. 3.2. It is to be noted that, as aforementioned as well as depicted in Fig. 3.2 a voltage regulator has been

incorporated for maintaining dc link dynamics within tolerable limit, where it receives an error signal resulting from the comparison between actual dc link voltage (V_{dc}) and corresponding reference voltage (V_{dcref})to generate appropriate output signal Z_2. Now, in order to generate controller output signal Z_1, in PI based damping controller, the controller block intakes speed deviation ($\Delta\omega$) as an error signal and then, yields suitable output signal Z_1. Similarly, lead-lag based damping controller also accepts $\Delta\omega$, and generates Z_1. It is to be noted that, since the transfer functions of these controllers are different, number of state variables generated by these controller blocks are different, too. For instance, number of associated state with PI controller is only one (Z_1), whereas, for lead-lag controller the number of associated states is three (Z_1, U_1, and U_2). Later, the combination of these two output signals Z_1, Z_2 with reference signal (δ_{Eref}) is delivered to a low-pass filter to generate effective control signal δ_E.

3.6 Optimization algorithms

In this section, a brief overview of the optimization methodologies that have been used in this research will be discussed. Generally, the aim of the optimization is to solve the problem of finding the parameters that maximize or minimize a given real- valued function [49]. It is to be noted that the detailed study of these algorithms are out of the scope for this work, and reader may consult to [50, 51, 52] for detailed study. In this research, the use of the optimization algorithms allows selecting optimal parameters that ensure the design for optimal damping controller.

3.6.1 Particle Swarm Optimization(PSO)

PSO is a novel population based metahuristic algorithm invented by Kennedy and Eberhart in 1995 [53]. PSO uses the social manners for instance, fish schooling and birds flocking to provide alternative solution to optimization problem from a given system generally non-linear in nature. The procedure that PSO follows is about sharing individual knowledge of fishes or birds originated from group communication during the period of migration or food searching. However, it is very common that the finest path of food searching will not be known to all and once it is identified by one member rest of the group follows that path.

In PSO, every individual from the population is known as a particle and the entire population is named as swarm. The algorithm begins with an arbitrarily introduced population and moves in arbitrarily selected route. Each particle remembers the previous best records of its own and neighbors during the period of crossing in the searching space. Particles of a swarm educate

better positions to one another as well as progressively alter their very own position and speed originated from the best position of whole particles. At whatever points every one of the particles have finished their development to another position, the subsequent stage starts. All particles in this manner will in general fly towards better positions over the searching procedure until the swarm go to an ideal position of the objective function.

Consider a search space of N-dimensional shape at the starting (N denotes the number of particle that needs to be optimized) and x_i^0 s are produced within the boundary limit

$x_{min} < x_i^0 < x_{max}$ where x_{min} and x_{max} are denoted as lower and upper boundary limit of the search region. Current fitness value are calculated from the initial fitness of x_i^0. It is to be mentioned that minimum current fitness values are recorded as personal best $j_{ind,i}^0$ whereas the lowest value of personal best is termed as global best $j_{best.}^0$ The position of particle corresponding to pbest and gbest is recorded as p_{best}^0 and g_{best}^0 respectfully. In the event that x_i^t indicates the position vector of particle *i* in the N-dimensional search space at time step , at that point the situation of every particle is modified from time to time in the search space according to equation [53].

$$v_i^{t+1} = v_i^t + c_1(pbest_i^t - x_i^t) + c_2(gbest_i^t - x_i^t) \quad (3.10)$$

$$x_i^{t+1} = x_i^t + v_i^{t+1} \quad (3.11)$$

Where, $x_{min} < x_i^0 < x_{max}$ and v_i^t is the velocity vector of particle *i* that drives the advancement procedure and reflects both individual and social experience information from every one of the particles. x_{min} and x_{max} are the separate lower and furthest points of boundary of the search space.

In this way, in a PSO strategy, all particles are started arbitrarily and assessed to process fitness together with finding the individual (best estimation of every particle) and global (best estimation of particle in the whole swarm). After that, a loop begins to locate an ideal position. Advancing first, the particles' speed is modified by the individual and global bests, and afterward every particle's position is updated by the present velocity. The loop is finished with a stopping criterion determined beforehand.

Steps of PSO algorithm:

Step 1: Define the problem space and set the boundaries.

Step 2: Initialize an array of particles with random positions and velocities inside the problem space.

Step 3: Check if the current position is inside the problem space or not. If not, adjust the positions so as to be inside the problem space.

Step 4: Evaluate the fitness of each particle.

Step 5: Compare the current fitness value with the particle's previous best value (pbest). If the current fitness value is better, assign the current value to pbest update the current coordinates.

Step 6: Determine the current global minimum among the molecule's best position (gbest).

Step 7: If the current global minimum is superior to gbest, employ the present value to gbest and update the current global best positions.

Step 8: Updatethe velocity as per condition (3.10).

Step 9: Move every particle to the new position as per condition (3.11) and go back to Step 3.

Step 10: Repeat Step 3 to Step 9 until the stopping criteria is fulfilled.

3.6.2 Grey Wolf Optimization (GWO)

Grey wolf has a place with canidae family. According to position, Grey wolves placed in the highest rank as predators, implying that they are at the top of the natural way of life. Grey wolves for the most part like to live in a pack. The bunch estimate is 5 ∼ 12 by and large. Specifically noteworthy is that they have a severe social predominant peck order.

The pioneers are a male and female, called alphas. The alpha is in the charge of decision making about chasing, time to wake and sleeping place for the most part. The alpha's choices are managed to the pack. However, some sort of popularity based conduct has too been watched, in which an alpha trails other members of the pack. In social occasions, the whole pack recognizes the alpha by holding their tails down. The alpha wolf is likewise called the predominant wolf since his/her requests ought to be trailed by the pack [54]. The alpha wolves are just permitted to mate in the pack. Strangely, the alpha isn't really the most grounded individual from the pack in any case, the best regarding dealing with the pack. This demonstrates the association and order of a pack is remarkably significant than its quality.

The second position in the hierarchy system of grey wolves is beta. The betas are subordinate wolves that help the alpha in basic leadership or the other pack activities. The beta wolf most

likely the best contender to be the alpha in the event that one of the alpha wolves passes away or turns out to be old. The beta fortifies the alpha's directions all through the pack and offers criticism to the alpha.

The most minimal positioning dim wolf is omega. The omega plays the job of substitute. Omega wolves dependably need to submit to all the other prevailing wolves. They are the last wolves that are permitted to eat. It might appear the omega isn't a significant individual in the pack, yet it has been seen that the entire pack face inner battling and issues if there should be an occurrence of losing the omega.

If a wolf is no longer alpha, beta, or omega, he/she is known as subordinate (or delta in some references). Delta wolves have to submit to alphas and betas, however, they dominate the omega. Scouts, sentinels, elders, hunters, and caretakers belong to this category [55].

Mathematical model of GWO algorithm:

In order to model the social hierarchy of wolves mathematically when designing GWO, the fittest solutions are considered as the alpha (α). Consequently, the second and third-best solutions are named beta (β) and delta (δ) respectively. The rest of the candidate solutions are assumed to be omega (ω). In the GWO algorithm the hunting (optimization) is guided by α, β, and δ. The ω wolves follow these three wolves [56].

The encircling behavior of the Grey wolf can be represented as follows

$$D = \left|\vec{C}.\overrightarrow{X_P}(t) - \vec{X}(t)\right| \tag{3.12}$$

$$\overrightarrow{X_{t+1}} = \overrightarrow{X_p}(t) - \vec{A}.\vec{D} \tag{3.13}$$

Where $\overrightarrow{X_P}$ denotes position vector of prey. $\vec{A}$ and $\vec{C}$ are coefficient vectors and $\vec{X}$ represents position vector of wolf. The coefficient vector $\vec{A}$ and $\vec{C}$ are calculated from the following equations.

$$\vec{A} = 2.\vec{a}.\overrightarrow{r_1} - \vec{a} \tag{3.14}$$

$$\vec{C} = 2.\overrightarrow{r_2} \tag{3.15}$$

Where, $\overrightarrow{r_1}$ and $\overrightarrow{r_2}$ are random vectors in [0 1]. Updated equations for velocity and position of best search agent are given as follows

$$\overrightarrow{D_\alpha} = \left| \overrightarrow{C_1} . \overrightarrow{X_\alpha} - \vec{X} \right|, \overrightarrow{D_\beta} = \left| \overrightarrow{C_2} . \overrightarrow{X_\beta} - \vec{X} \right|, \overrightarrow{D_\delta} = \left| \overrightarrow{C_3} . \overrightarrow{X_\delta} - \vec{X} \right| \quad (3.16)$$

$$\overrightarrow{X_1} = \overrightarrow{X_\alpha} - \overrightarrow{A_1}. \overrightarrow{D_\alpha}, \overrightarrow{X_2} = \overrightarrow{X_\beta} - \overrightarrow{A_2}. \overrightarrow{D_\beta}, \overrightarrow{X_3} = \overrightarrow{X_\delta} - \overrightarrow{A_3}. \overrightarrow{D_\delta} \quad (3.17)$$

$$\overrightarrow{X}(t+1) = \frac{\overrightarrow{X_1} + \overrightarrow{X_2} + \overrightarrow{X_3}}{3} \quad (3.18)$$

Outline of GWO algorithm:

Step-1: Initialization:

Initialize the main population of grey wolf randomly, figure their fitness and discover the best wolf as alpha, second best as beta and third best as delta. The remainder of wolf expected as omega.

Step-2: To update the position of grey wolf:

The situation of the wolf is modified time to time on the basis of the location of three wolfs (alpha, beta and delta).

Step -3: Replacing the present position with the better one:

Update the position of alpha, beta or delta if new position of wolf has better fitness.

Step-4: To check the stopping criterion of the algorithm:

If end criterion is fulfilled, return the alpha as the best solution for given issue. Again if find something different, back to refresh wolf position steps.

3.6.3 Differential Evolution (DE) algorithm

DE is one of the types of progressive algorithm group which has striking properties of resolving optimization complications. The elementary DE algorithm was first suggested by Storn and Price in 1997 [57]. The main steps of DE algorithm are initialization of a group of clarification, secondly mutation, then recombination and finally selection. Various steps related to DE algorithm are discussed below:

Step 1: In this step which is called initialization phase, an arbitrary set of probable solution for each component is engendered within the search space. If an objection function having D real parameters is to be adjusted for an primary population of size NP, the parameters vector includes the for $X_{i,G} = [X_{1,i,G} X_{2,i,G} \ldots\ldots\ldots X_{D,i,G}]$ with i= 1, 2,... NP, where G is the

generation number. With the maximum and minimum limits for each parameter noted as $x_j^L \leq X_{j,i,1} \leq x_j^U$, where he arbitrary parameters in each generation should lie within the interval [x_j^L , x_j^U].

Step 2: Three target vectors $x_{r1,G}$, $x_{r2,G}$ and $x_{r3,G}$ are arbitrarily nominated from a specified parameter vector (x_i,G) for the mutation phase keeping in notice that the keys r_1, r_2 , r_3 and i are different. These three vectors with mutation factor MF are used to produce the donor vector following the strategy as [57]

$$V_{i,G+1} = x_{r1,G} + M_F(X_{r2,G} - X_{r3,G}) \tag{3.19}$$

Alternative method of making the donor vector $V_{i,G+1}$ is to follow the current best value which integrates the consequence of overall best of each generation as [57]:

$$V_{i,G+1} = x_{i,G} + M_F\left(x_{r2,G} - x_{r3,G}\right) + \lambda\left(x_{best,G} - x_{i,G}\right) \tag{3.20}$$

Here, the second mutation operator is λ. In this thesis, eq. (3.19) is employed for the mutation phase.

Step 3: Phase trial vector denoted by $V_{j,i,G+1}$ is generated in the recombination which gets updated by the donor vector which has probability CR.

$$V_{j,i,G+1} = \begin{cases} V_{j,i,G+1}, & if\ r\ and\ j,i \leq C_R\ or\ j = I_{Tand} \\ V_{j,i,G}, & if\ r\ and\ j,i \leq C_R\ or\ j = I_{Tand} \end{cases} \tag{3.21}$$

r and *j* ,*i* is an arbitrary number having the range within [0,1] and I_{Tand} is a random integer which is taken from [1,2,. . . ,D].

Step 4: In the selection step, an evaluation is made between the objective vector and preliminary vector and the ones with the best value is chosen and sent to the generation to repeat.

$$x_{i,G+1} = u_{i,G+1}\ if\ j\left(u_{i,G+1}\right) \leq j(\ x_{i,G}\ ) \tag{3.22}$$

$$x_{i,G} \qquad \text{otherwise}$$

The mutation, recombination and selection stages proceed until a pre-indicated stopping basis is satisfied.

3.7 Objective functions

To enhance power system stability, the optimal stabilizer parameters are chosen to optimize objective function *J* formulated from a given problem, subject to inequality constraints, which are the limits of each controller gain K and time constants $T1$–$T4$. In this work, two eigenvalue based objective functions have been considered for the controller design problem. Eigenvalue-based objective function is given as

$$J_1 = \sum_{i=1}^{n} (\sigma_i - \sigma_0)^2 \tag{3.23}$$

$$J_2 = \sum_{i=1}^{n} (\zeta_0 - \zeta_i)^2 \tag{3.24}$$

$$J = -(J_1 + \omega J_2) \tag{3.25}$$

Here, σ_i is the real part of the i_{th} eigenvalues, $\sigma_0$is the ideal estimation of the real part of the eigenvalues, ζ_i and $\zeta_0$are the real and actual estimations of the damping proportions individually and ω is the weighting factor which is taken as 0.1 in this thesis work. Optimization of J_1 will guarantee that the real part of the eigenvalues are lying in the stable position and that of J_2 will ensure that adequate damping has been infused to the system elements.

In this way, minimization of J will guarantee that both J_1 and J_2 are satisfied simultaneously while an optimization arrangement of controller gains is acquired. It is aimed to enhance system damping. In other words it is aimed to minimize this objective function to reduce the weighted speed deviation.

Therefore, in order to depict the optimization problem, constraints of the parameter can be represented as: Optimize J Subject to the constraints of the parameters of the Lead-Lag controller and PI controller are as follows

$$K^{min} \leq K \leq K^{max} \qquad K_{p1}^{min} \leq K_{p1} \leq K_{p1}^{max}$$

$$T_1^{min} \leq T_1 \leq T_1^{max} \qquad K_{i1}^{min} \leq K_{i1} \leq K_{i1}^{max}$$

$$T_2^{min} \leq T_2 \leq T_2^{max} \qquad K_{p2}^{min} \leq K_{p2} \leq K_{p2}^{max}$$

$$T_3^{min} \leq T_3 \leq T_3^{max} \qquad K_{i2}^{min} \leq K_{i2} \leq K_{i2}^{max}$$

$$T_4^{min} \leq T_4 \leq T_4^{max}$$

In this research work, optimization approaches have been carried out using the above mentioned constraints.

3.8 Controller parameter optimization

Optimization is characterized as the way toward finding the conditions that give the base or most extreme condition of a function, where the function expresses the effort required. It is effectual to use optimization algorithm for a system when controlling is manipulated by random variables. Basically optimization refers to maximize or minimize an objective function subjected to some specific constraints. The main goal of employing optimization algorithm is to select the optimal parameters among the different options to operate system in optimal conditions. In proposed damping controller design, three different optimizers such as PSO, DE and GWO are resorted to tune the PI and Lead-Lag damping controller for the enhancement of damping ratio. In the organization of this section firstly fundamental procedure of the mentioned optimizers will be discussed then the research work scenario will be discussed.

As aforementioned, since selection of appropriate gain (K, K_{p1}, K_{i1}, K_p, K_i) and time constants $(T_1 - T_4)$ for corresponding controllers yield their best output responses, here, in this work, three different optimization algorithms such as PSO, DE, and GWO are resorted to tune these constants, since improper tuning may lead to sub-optimal outcomes. Now, in order to perform above mentioned optimizations, at first, definition of the parameters are needed for these algorithms. However, since the optimization method for these algorithms are different, they have some similar as well as dissimilar parameters that need to be defined. For instance, maximum

population size (100), maximum number of iteration (100), number of runs (30) are listed as similar parameters whereas, for PSO, cognitive accelerating coefficient (2) and social accelerating coefficient (1.5) for DE, mutation factor (0.9), crossover probability (0.2); for GWO, range of weighting factor for prey [2,0] are itemized as dissimilar parameters, which are considered for this work. After defining the parameters for our optimization algorithms, to keep the search space within practically feasible limits for these optimization algorithms, we restrict the controller parameters by defining upper and lower bounds.

In this work, (100, 0.1) for K, K_{p1}, K_{i1}, K_p, K_i and (2, 0.1) are considered for time constant parameters (i.e. $T_1 - T_4$) as upper and lower bound respectively. Additionally, in order to perform optimization using these algorithms, an eigenvalue based objective function is resorted cited in [58], whose minimization will ensure our desired optimal control parameters. It is to be noted that, eigenvalue based objective function exhibits better performance than time domain based objective function in terms of computational time [59]. Furthermore, to find the preeminent optimization algorithm among these three, we compare their performances in terms of elapsed time and best fitness value obtained from multiple runs (30).

3.9 Time domain analysis

One of the most accurate ways to study LFO problem is time domain analysis where consideration of the approximation in the DAE model is ignored. However, time do- main simulation lacks some features such as relevant information regarding various weak modes, the overriding states variable associated with weak modes and response of those modes to parameter variation and other details. Hence, it is suggested for small signal stability analysis to perform eigenvalue and time domain analyses, where it is utilized as reciprocal answers for help one another and confirm the outcomes.

In time domain analysis, mode is perturbed and the behavior of state variable is calculated by solving differential equations using some numerical integration techniques with the known initial values [60, 61, 62]. The initial values in this case, are the initial equilibrium point. In this research work, both eigenvalue and time domain analyses have been used. It is to be noted that dynamic characteristics of the state such that peak overshoot, peak undershoot, settling time can be perceived easily from time domain analysis. When a system is subjected to small disturbance it experiences transient reaction which is connected with a oscillation, which might be sustained or decaying in nature. The certain behavior of the system relies on the parameters

of the system. Since any system can be modeled with a direct differential condition, the arrangement of this direct differential condition gives the reaction of the system. From the time domain simulation it is seen that, dynamic responses are started at the instant of disturbance and oscillation sustains for a specific period until adequate damping is provided.

3.10 Non-parametric statistical test

Here, in this work, non-parametric statistical test is employed such as Kolmogorov- Smirnov and Paired sample *t*-test to identify presence of significant non-uniformity among above mentioned optimizers. For this purpose, each of the optimizers was run several times (30) to obtain corresponding fitness values and to supply these fitness values as input to IBM SPSS (version *23)* software. In case of Kolmogorov- Smirnov test, to identify the nature of data-set distribution, two hypotheses such as, H_0, the null hypothesis, accepts the data set agreed with normal distribution whereas, H_1, the alternate hypothesis, rejects the decision of H_0 with 5% significance level are employed [63]. Nevertheless, for Paired sample *t*-test, to justify the statistically significant correlations among data-set, moreover, two hypotheses based on Asymp. Sig. 2-tailed value (i.e. *p*-value); the null hypothesis H_0, accepts if the data sets are correlated and the alternative hypothesis H_1, admits if the data sets are different with a significance level of 0.05 are considered.

3.11 Data set for GUPFC equipped SMIB system

To carry out the analysis of the system performance the following data table is adopted for this research work [5, 6].

Table 3.3 Data set for the study system

Generator data		
x_d = 1 *p.u.*	x_q = 0.6 *p.u.*	x'_d = 0. 3 *p.u.*
D = 0 *p.u.*	M = 8 *MJ/MV A*	T'_{do} = 5:044 *p.u.*
Exciter system		
K_A=100	T_A=0.01 *sec.*	
Transformer data		
X_T=0.25 *p.u.*	X_A=0.1 *p.u.*	X_B= 0.1 *p.u.*
X_E=0.50 *p.u.*		
Network data		
X_{AV}=0.1 *p.u.*	X_{BV}=0.1 *p.u.*	
GUPFC data		
m_E=0.9990 *p.u.*	m_A=0.8084 *p.u.*	m_B= 0.8084 *p.u.*
δ_E=-115.18°	δ_A=-37.10°	δ_B=-37.10°
dc regulator data		
K_p=80	K_i=10	
dc link data		
V_{dc}=2 *p.u.*	C_{dc}=1 *p.u.*	

Chapter 4
Analysis of GUPFC

In this chapter, employing pre-defined parameter for each of the optimizers discussed in the section 3.8, optimal values for the controller parameters (i.e. gain and time constants) of PI and Lead-Lag is obtained which is discussed in section 4.1. Later, these optimal data are adopted for analyzing close-loop eigenvalue and time-domain simulation for various loading condition such as nominal, light and heavy load which is discussed in section 4.2 and 4.3 respectively. Finally, to discern the statistical behavior of the optimizer clearly non-parametric test results has been discussed in the end of this chapter.

4.1 Controller parameter optimization results

The main goal of employing optimization algorithm is to select the optimal parameters from the different options to operate system in optimal conditions. In proposed damping controller design, three different optimizer such as PSO, DE and GWO are resorted to tune the PI and Lead-Lag damping controller for the enhancement of damping ratio. In this work, (100, .01) for K, K_{p1}, K_{i1}, K_p, K_i and (2, .01) are considered for time constant parameters (i.e. T_1-T_4) as upper and lower bound respectively. Additionally, in order to perform optimization using these algorithms, an eigenvalue based objective function is resorted cited in [58], whose minimization will ensure desired optimal control parameters [6, 7]. In this research work the optimal control parameters obtained from the optimization algorithm are listed in Table 4.1.

Table 4.1: Optimized parameters obtained using PSO, DE, and GWO

Controller	Parameters	PSO	DE	GWO
PI	K_{p1}	4.9543	3.5214	4.08353
	K_{i1}	5.1884	2.9100	3.28452
	K_p	63.1940	79.6421	79.0321
	K_i	30.0574	0.3284	11.2126
Lead-lag	K	80.1116	99.7887	99.5721
	T_1	0.0177	0.02157	.0224
	T_2	0.01	0.01	0.01
	T_3	4.1938	3.24159	3.2890
	T_4	3.7869	1.6377	1.7819

It is to be noted from the table presented in Table 4.1 that except lag time constant, T_2 all optimal values corresponding to each optimization algorithm are lying within defined search space. This implies that search space to select optimal control parameters considered for this system are significantly accurate. Moreover, these optimal values listed in Table 4.1 are correlated with best elapsed time and fitness value for that particular optimizer, which will be discussed later in the section of quantitative analysis.

4.2 Eigenvalue analysis in close-loop

Here, in this section, using the data of Table 3.4, eigenvalue analysis of state matrix, *A* for both PI and Lead-Lag controller based close-loop system have been presented, where GWO, DE and PSO have been used as optimizers to tune these controllers. The outcomes of the above analysis are listed in Table 4.2 and 4.3 respectively, where, it is obvious that all the eigenvalues are shifted significantly toward the left half of *S*-plane for both controllers compared to open-loop eigenvalue of corresponding associated state presented in Table 3.3, which signifies the overall stability of close-loop system. More precisely, concerned unstable mode from open-loop analysis (i.e. δ - ω) which had positive real value of 0.0682, possess negative real value in close-loop system.

Table 4.2: Analysis of eigenvalue with PI integrated controller

State	GWO	DE	PSO
E_{fd}	-85.4163	-85.4164	-85.2414
$\acute{E_q}$	-15.7053	-15.6953	-15.6649
V_{dc}	-2.0251	-1.7271	-3.8959
δ, ω	-5.3751 ± 5.4613i	-4.9910 ± 5.2171i	-3.7356 ± 4.1752i
δ_E,Z_2	-3.5160	-4.5796	-4.1297 ±0.1920i
	-3.1425	-3.1379	
Z_1	-2.9247e - 15	-1.5587e - 15	-1.8905e – 15

For PI controller, with GWO, DE, and PSO tuned, eigenvalue associated with δ - ω have the real part of -5.3751, -4.9910 and -3.7356 with damping ratio of 0.0915, 0.0957, and 0.1190

respectively.

Again for Lead-Lag controller, the real part of the eigenvalue associated with δ - ω are -3.2696, -3.3659, and -2.8893 with damping ratio of 0.2237, 0.2219, and 0.1967 respectively for each of the tuning algorithms GWO, DE, and PSO. It is observed that damping ratio (-0.0019) of negatively damped unstable mode associated with δ - ω obtained in open-loop analysis are improved for all the cases in close-loop system, and more particularly, the improvement is superior for GWO algorithm of Lead-Lag controller.

Table 4.3: Analysis of eigenvalue with Lead-Lag integrated controller.

State	**GWO**	**DE**	**PSO**
E_{fd}	-98.7011	-98.7011	-98.7015
$\acute{E_q}$	-1.6635	-1.6792	-1.8816
V_{dc}	-0.8607	-0.7623	±0:3108i
δ, ω	-3.2696 ± 1.9817i	-3.3659 ± 1.9597i	-2.8893 ± 2.5179i
δ_E,Z_2	-8.4310 ± -7.3652	-7.7553 ±1.2114i	-6.9357 ±1.8862i
Z_1U_2	-98.4864 ±14.8565i	-98.5743 ± 13.8422i	99.2091 ± 8.1940i
U_1	-0.1995	-0.1994	-0.1998

Additionally, in open-loop analysis, eigenvalue associated with dc link voltage is -0.0685, whereas, under close-loop scenario for both the controllers. It is observed from Table 4.2 and 4.3 respectively, the corresponding eigenvalues in all cases are shifted toward the left half of the s-plane and it is the largest for PI controller tuned with GWO. Now, in order to find the best condition from close loop eigenvalue analysis, it is quite challenging to comment on overall performance of the optimizers as well as controllers in term of mitigating LFO, since eigenvalue corresponding to different states are dissimilar. Hence, time-domain simulation is carried out to find the best combination of controller along with its associated tuning algorithm, which will provide comparatively better damping effect in mitigating LFO for close-loop system.

4.3 Time-domain simulation result

To perform time domain simulation, a small perturbation is introduced to the study system by employing sudden mechanical input changes after 0.1 second of the starting of the simulation with a step change of 0.1 *p.u.* in order to analyze the performance of the tuned controllers by observing the nature of speed deviation in terms of overshoot, undershoot, and settling time. It is to be noted that, we perform time domain simulation for nominal load (P_e = 0.85 *p.u.*, Q = 0.115 *p.u.*), light load (P_e = 0.3 *p.u.*, Q = 0.015 *p.u.*), and heavy load (P_e = 1.2 *p.u.*, Q = 0.4 *p.u.*) to validate the effectiveness of tuned controllers, since consideration of such loading conditions are more practical and hence, are widely adopted in the literature [34]. Now, considering these loading conditions, results of the time domain simulation for tuned PI and lead lag controller have been depicted in Fig. 4.1 to Fig. 4.6 respectively.

In case of PI based damping controller of Fig. (4.1-4.3), it is observed that under nominal load condition, the peak overshoot (OS) for GWO (0.00135 *p.u.*) are least among these three optimizers. Like nominal load condition, OS of GWO for heavy load (0.0013 *p.u.*) and for light load (0.0015 *p.u*) are smaller compared to DE and PSO. The settling time of GWO, DE, and PSO are 1.6590 *sec.*, 1.6137 *sec.* and 1.5520 *sec.* respectively under nominal load condition. For heavy load scenario settling time recorded are 1.6236 *sec.*, 1.6138 *sec.*, and 1.6088 *sec.* respectively. Similarly the settling time of GWO, DE and PSO are 1.8339 *sec.*, 1.8318 *sec.*, and 1.8388 *sec*. respectively under light load condition. It is observed that although under nominal load GWO requires a bit longer settling time than PSO and DE, it is almost identical for heavy and light load for all three algorithms. Hence, for PI based controller, GWO exhibits best performance in term of OS with the sacrifice of a bit of settling time under all loading scenarios.

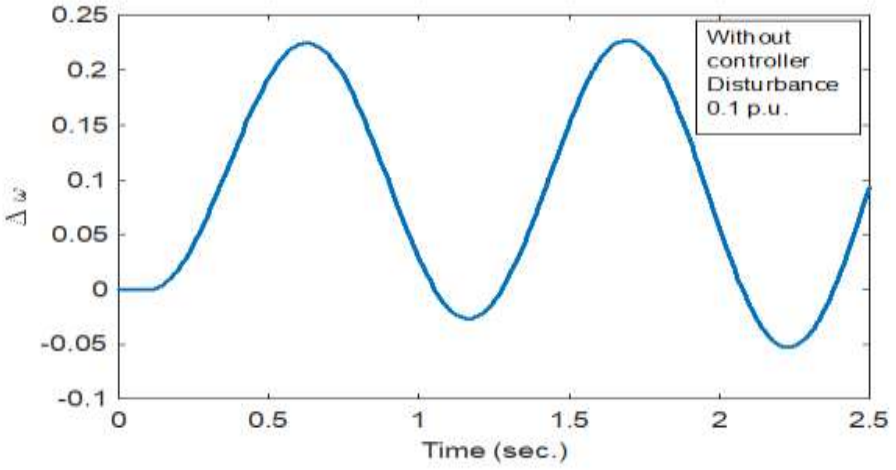

(a)

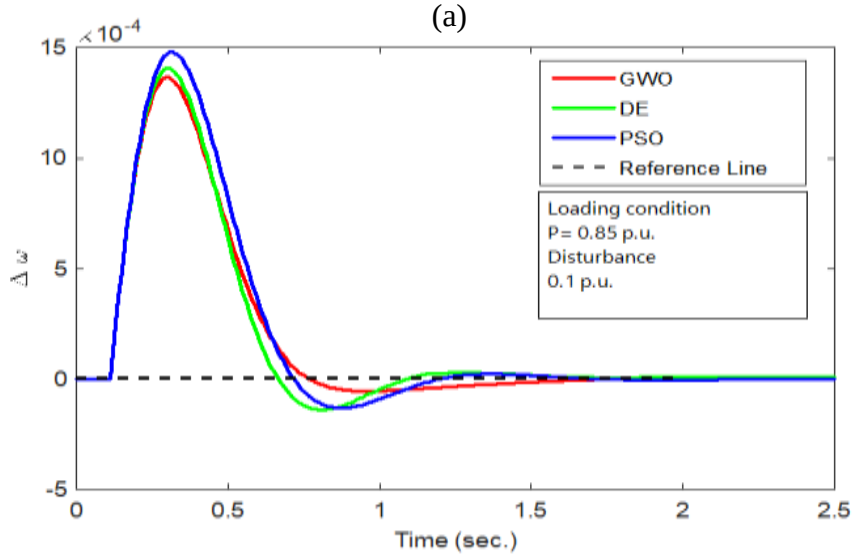

(b)

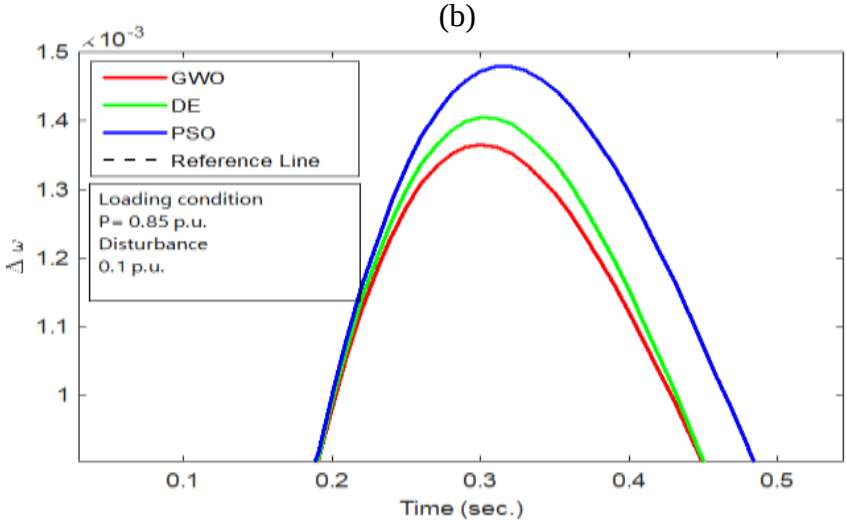

(c)

Figure 4.1: Time-domain simulation for nominal load condition with PI controller: (a) without controller (b) comparison of different optimizer (c) zoom view of overshoot

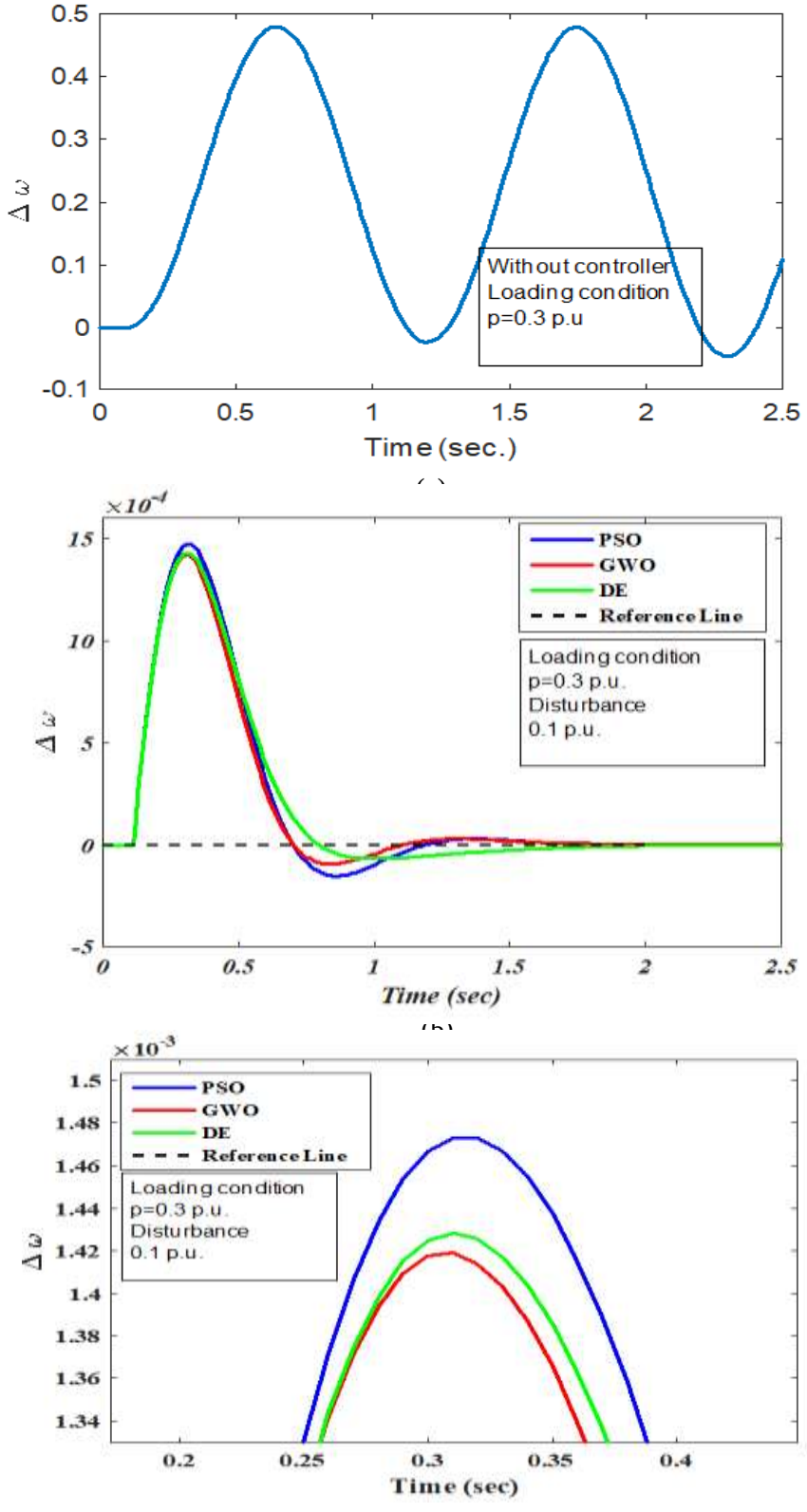

(c)

Figure 4.2: Time-domain simulation for light load condition with PI controller: (a) without controller (b) comparison of different optimizer (c) zoom view of overshoot

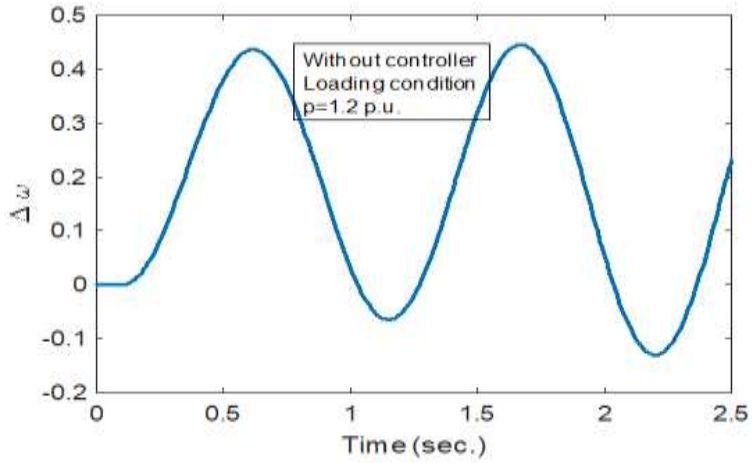

(a)

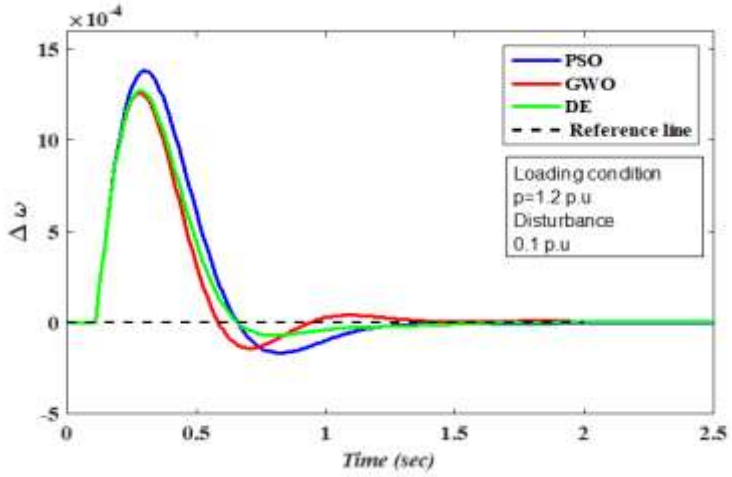

(b)

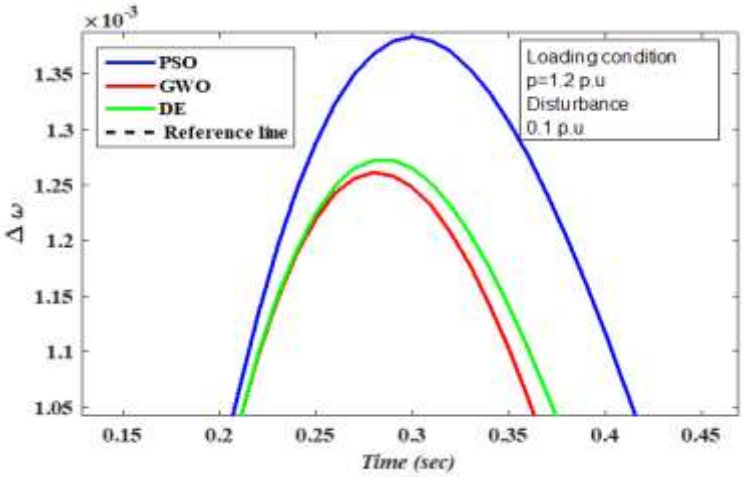

(c)

Figure 4.3: Time-domain simulation for heavy load condition with PI controller: (a) without controller (b) comparison of different optimizer (c) zoom view of overshoot

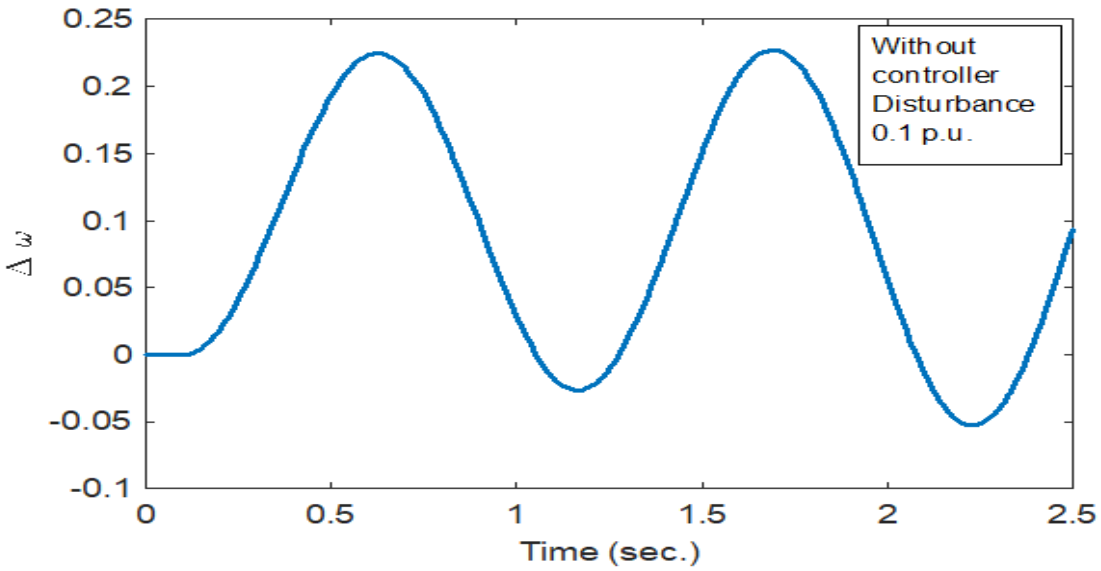

(a)

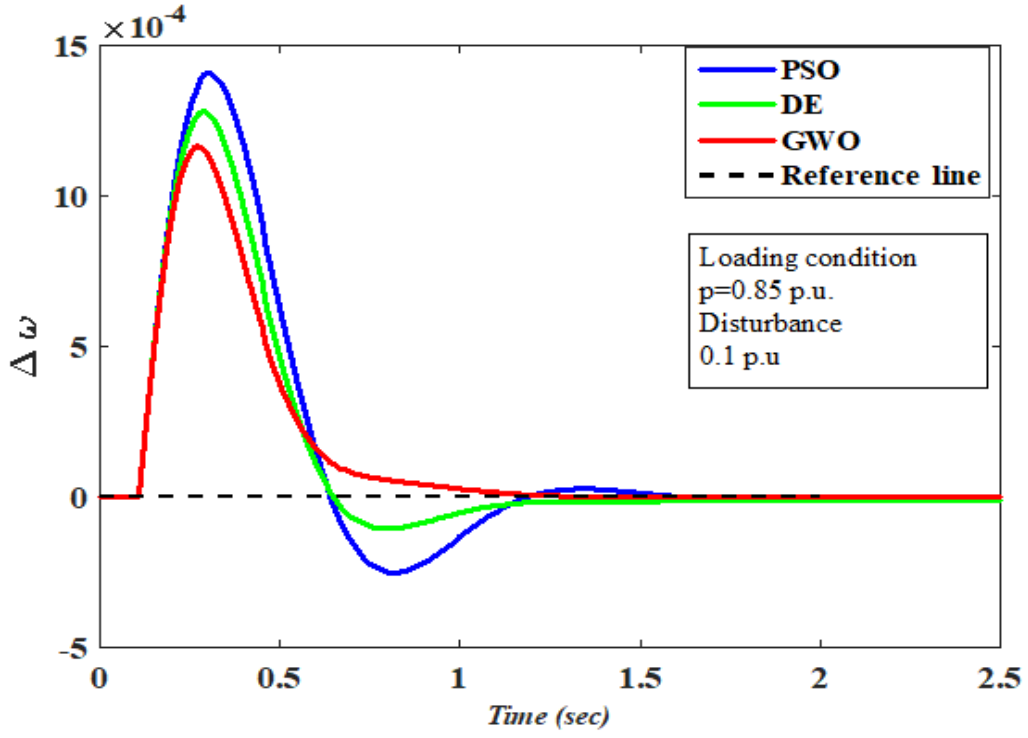

(b)

Figure 4.4: Time-domain simulation for heavy load condition with Lead-Lag controller: (a) without controller (b) comparison of different optimizer

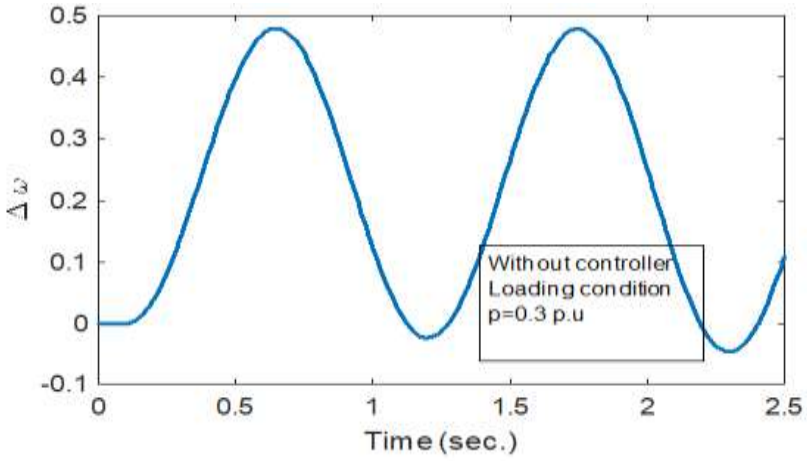

(a)

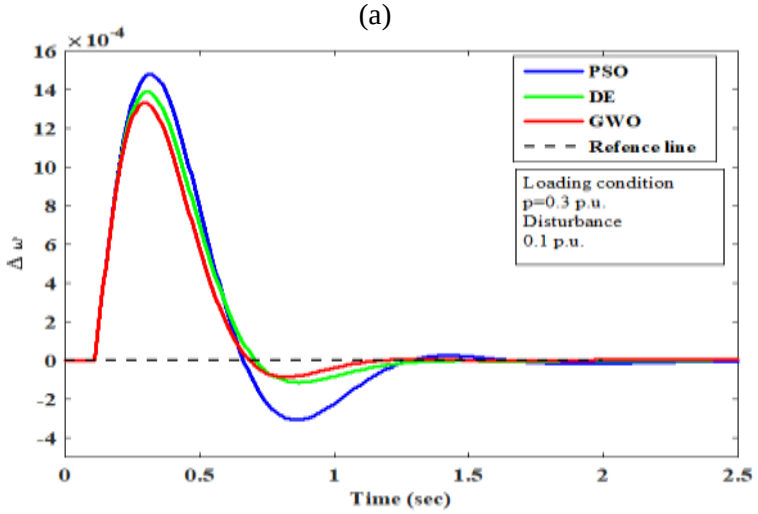

(b)

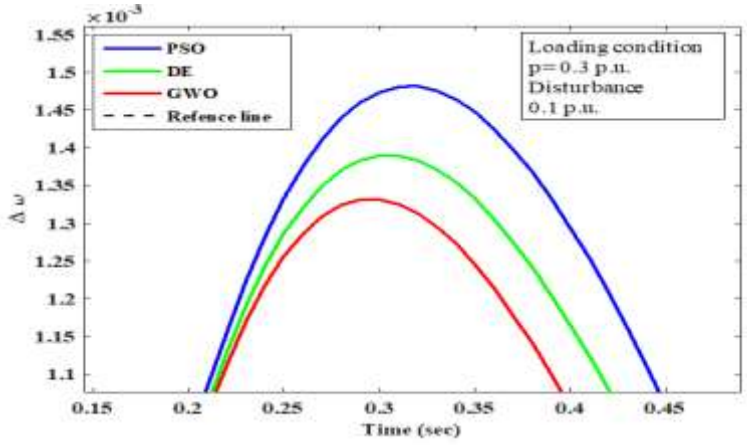

(c)

Figure 4.5: Time-domain simulation for light load condition with Lead-Lag controller: (a) without controller (b) comparison of different optimizer (c) zoom view of overshoot

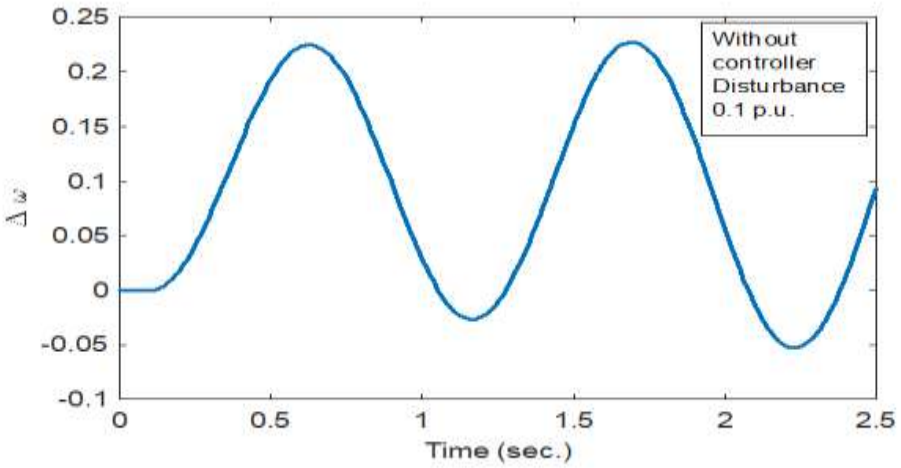

(a)

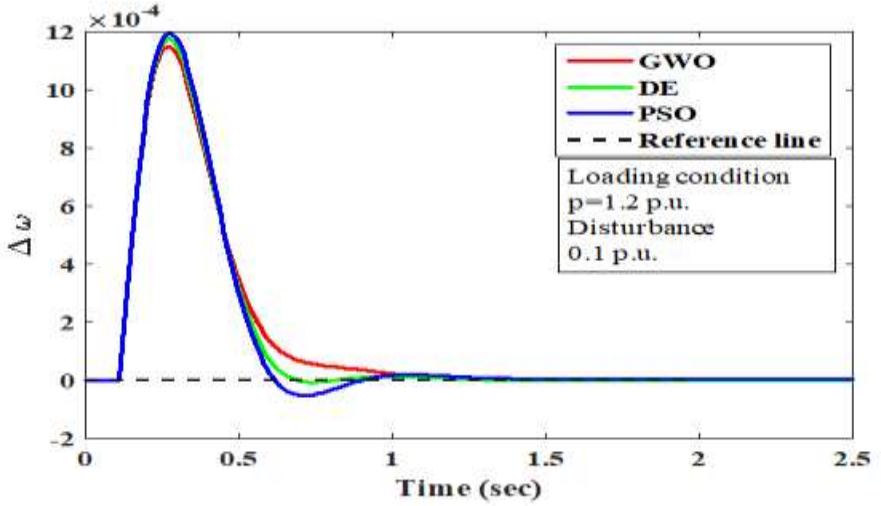

(b)

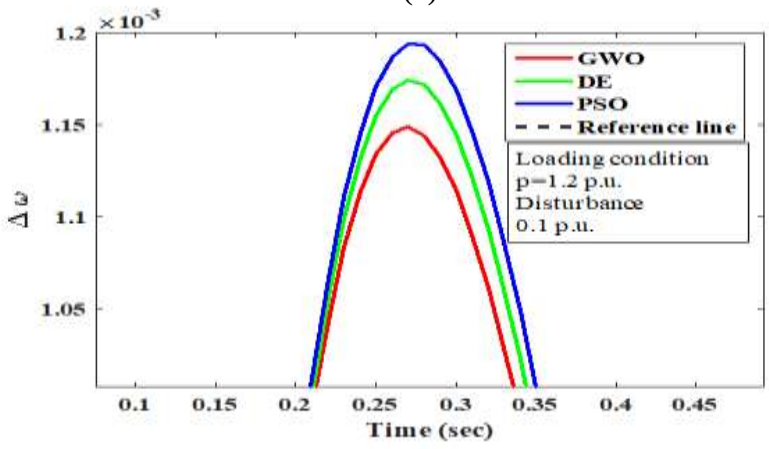

(c)

Figure 4.6: Time-domain simulation for heavy load condition with Lead-Lag controller: (a) without controller (b) comparison of different optimizer (c) zoom view of overshoot

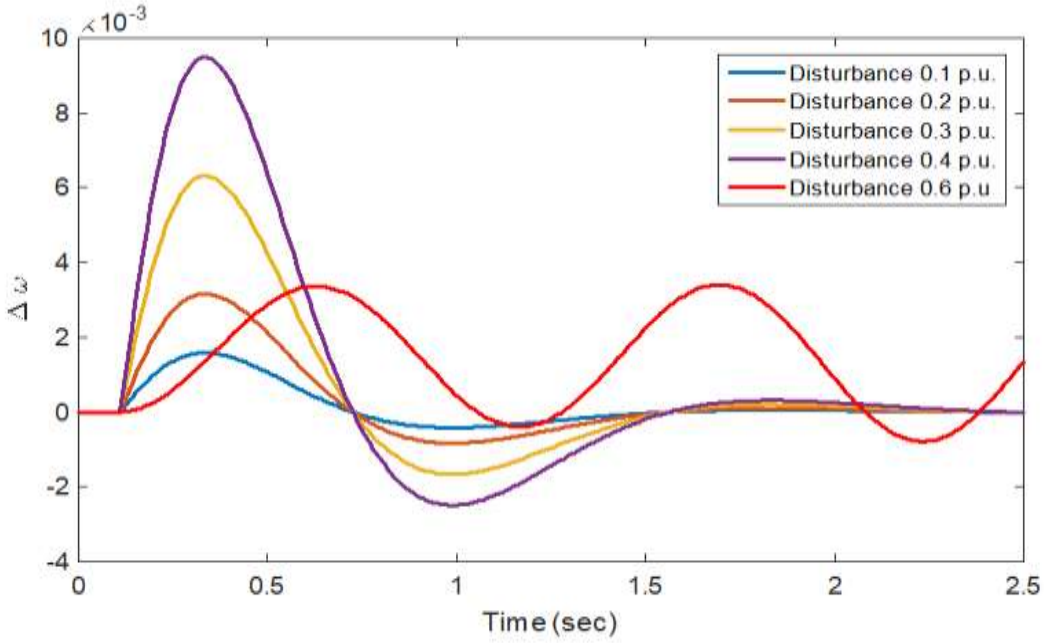

(a)

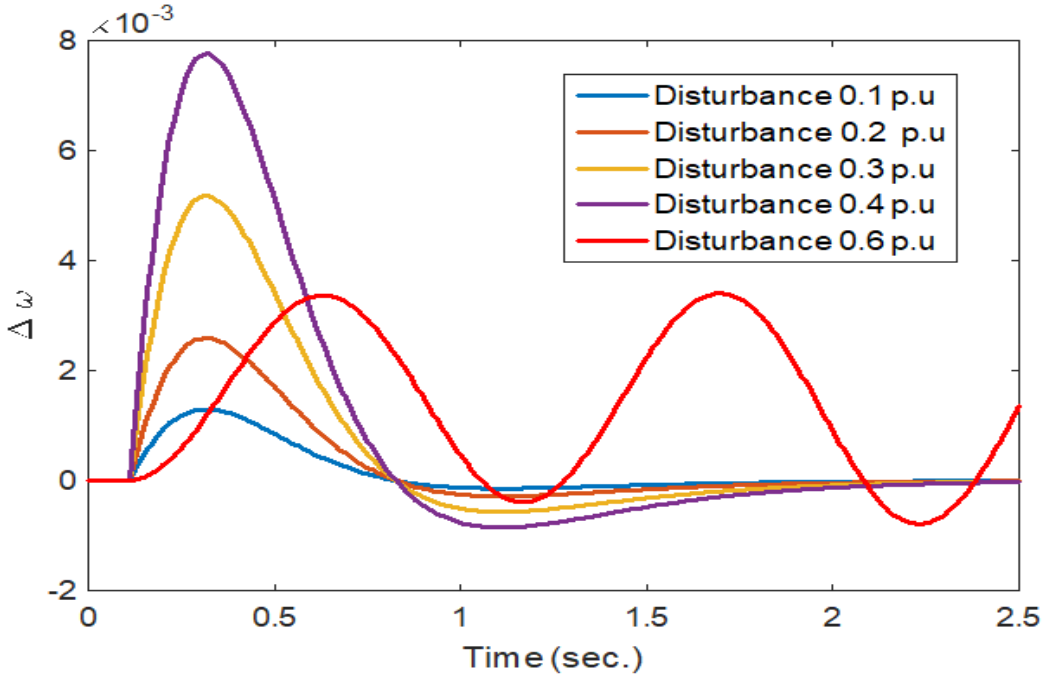

(b)

Figure 4.7: Effect of different disturbance for nominal load condition with (a) PI controller (b) Lead-Lag controller

Now, in case of Lead-Lag controller, it is illustrated from Fig. (4.4-4.6) that, GWO shows better performance in terms of OS under nominal (0.0013 *p.u.*), heavy (0.0012 *p.u.*), and light load (0.0014 *p.u.*) respectively than DE, and PSO. The settling time reported for GWO, DE, and PSO are 1.8630 *sec.*, 1.8576 *sec.*, and 1.7325 *sec.* respectively for nominal load. In case of heavy load, settling time recorded for GWO, DE, and PSO are 1.8374 *sec.* 1.8316 *sec.*, and 1.8021 *sec.* respectively. Similarly settling time recorded for light load condition are 2.1020 *sec.*, 2.1007 *sec.*, and 1.9231 *sec.* respectively. It is revealed that, GWO and DE exhibit almost similar settling time and a little extent greater than PSO. Like PI based damping controller, in case of Lead-Lag based controller, GWO demonstrates better performance in term of OS with a bit longer settling time than those of DE, and PSO. Here, it is to be noted that GWO tuned Lead-Lag controller exhibits better performance than GWO tuned PI controller considering OS. Hence, GWO tuned Lead-Lag controller may be selected with compromising a bit of settling time.

Again, in order to validate the effectiveness of the damping controller under the study system, step size disturbance with varying magnitude has been employed. The result shown in Fig. 4.7 (a) and 4.7 (b) reveals that with the increase of the strength of disturbance overshoot increases and unable to control for a particular operating condition. In this research, it is observed that the designed GUPFC based damping controller can sustain the disturbance level within a specific operating condition. Level of disturbance exceeding 0.6 *p.u*. makes the system unstable which supports the approach of the linearized model.

4.4 Quantitative analysis

In this section, quantitative analysis is performed among these optimizers for both controllers in order to find out diversity among them, since each of these optimizers deal with certain level of probability and likelihood. The outcomes of the quantitative analysis among these optimizers in terms of computational time i.e. best, average, and worst elapsed time are illustrated in Fig 4.8. It is revealed from the figure that GWO needs least computational time for PI and Lead-Lag based controller than DE, and PSO. For best case, the computational times are 1.5072 *sec.* for PI and 1.6758 *sec.* for Lead-Lag, for average case, the computational times are 1.5320 *sec.* for PI and 1. 6843 *sec.* for Lead-Lag, and for worst case these times are 1.575 *sec* for PI and 1.7051 *sec* for Lead-Lag. Now, in the calculation for fitness value, GWO and DE exhibit almost identical magnitude compared to PSO for both types of controllers.

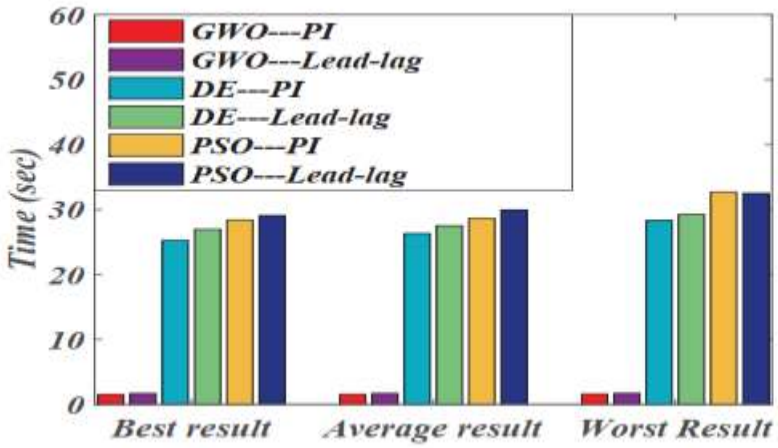

Figure 4.8: Elapsed time comparison among different controller-optimizer pairs

The calculated fitness values of GWO and DE are -34325.20 for PI and -177654.6262 for Lead-Lag in best case; -34324.76 for PI and -177651.4716 for Lead-Lag in average case; -34324.44 for PI and -177648.3171 for Lead-Lag in worst case. Hence, it is revealed that GWO is better for PI and Lead-Lag controller in terms of both elapsed time and fitness value, which supports the result obtained in time-domain simulation.

4.5 Non-Parametric statistical analysis

As mentioned in previous section, to figure out statistically substantial difference among different optimizers and as well as to strengthen the conclusion obtained from time domain simulation and quantitative analysis, one sample Kolmogorov-Smirnov (KS) test and paired sample t-test for 30 independent test runs are carried out and the data sets are presented in Table 4.3, 4.4, and 4.5 respectively.

Table 4.4: Single Sample Kolmogorov-Smirnov test results for PI controller

Statistical Parameters		**PI controller**		
		GWO	**DE**	**PSO**
Mean		−34324.77	−34324.53	−34321.10
Standard Deviation		0.33	0.32	1.70
Most Extreme Differences	**Absolute**	0.293	0.149	0.087
	Positive	0.206	0.149	0.087
	Negative	−0.293	−0.108	−0.066
Kolmogorov-Smirnov Z		1.605	0.817	0.476
Asymp. Sig. (2-Tailed)		0.012	0.518	0.976

Table 4.5: Single Sample Kolmogorov-Smirnov test results for Lead-Lag controller

Statistical Parameters		Lead-Lag controller		
		GWO	**DE**	**PSO**
Mean		−177651.54	−177651.51	−177637.8227
Standard Deviation		8.45	1.65	6.6316
Most Extreme Differences	**Absolute**	0.410	0.183	0.299
	Positive	0.410	0.080	0.299
	Negative	−0.306	−0.183	−0.206
Kolmogorov-Smirnov Z		2.246	1.004	1.635
Asymp. Sig. (2-Tailed)		0.000	0.266	0.010

From Table 4.5, it is noticed that in case of PI controller, mean value (-34324.77) of GWO outperforms the mean value of DE (-34324.53) and PSO (-34321.10). Again, in terms of standard deviation, GWO and DE show almost identical performance, which is better than PSO. Now, in case of Lead-Lag controller, similar sort of performance is observed for DE and GWO in term of mean value, which is better than that of PSO. Again, in term of standard deviation, DE (1.65) outperforms the standard deviation of PSO (6.6316) and GWO (8.45). Furthermore, the *p* value (Asymp. Sig.2-tailed) presented in the table V shows that for PI controller, GWO (0.012) accepts H_1, implies that it does not follow normal distribution, whereas, DE and PSO are unable to show significant results to support H_1 , and hence, they reject H_1 and accept H_0. Therefore, it can be concluded that GWO data are dissimilar from DE and PSO with 95% confidence level. Again, for Lead-Lag based controller, the *p* value (Asymp. Sig.2-tailed) for GWO (0.000) and PSO (0.010) accepts H_1, implies that they do not follow normal distribution, whereas, DE (0.266) reject H_1 and accepts H_0. Therefore, it can be concluded that data sets of GWO and PSO are dissimilar from DE with 95% confidence level.

Table 4.6: Paired sample *t* test results

Controller	Method	Pair differences				
		Mean	**Correlation**	t	df	**Sig. (2-tailed)**
PI	**DE-PSO**	−3.4270	−0.70	−10.711	29	0.000
	DE-GWO	0.2392	0.143	3.085	29	0.004
	PSO-GWO	3.6662	0.130	11.883	29	0.000
Lead-lag	**DE-PSO**	−13.71794	−0.159	−10.608	29	0.000
	DE-GWO	0.06905	−0.0391	−0.041	29	0.968
	PSO-GWO	−13.6488	−0.172	−6.444	29	0.000

Again, from the Paired sample *t - test* presented in Table 5, it is observed that Asymp. Sig. 2 tailed value of the three pairs lies below 0.05 for PI based controller; hence, these reject H_0 that indicates the uniqueness of the data. Similar types of remarks can be drawn after investigating the statistical performance of the optimizers for lead lag controller barring some similarities obtained for DE-GWO pair of data, since the value of Sig. 2-tailed lies above 0.05.

Chapter 5

Conclusion and Recommendations for the Future Works

5.1 Conclusion

In this work, a comprehensive study between two conventional damping controller such as PI and Lead-Lag controller for a third generation FACTS device (i.e. GUPFC) is presented in order to provide damping for mitigating LFO in an SMIB system. With this aim, at first eigenvalue analysis has been conducted in open loop condition to demonstrate the feasibility of incorporation of controller and to find the unstable mode (EM mode). Then, optimized PI and Lead-Lag controller are incorporated separately to the system, which improves the negatively damped EM (-0.0019) mode noticeably by shifting all the eigenvalues to the left half of S-plane. It is to be noted that, for optimization of both the controllers, three different algorithms are adopted such as GWO, DE, and PSO. Later, the settling time and overshoot have been investigated through time domain simulation in order to figure out the best combination of controller-optimizer pair for the system. Comparative study reveals that to mitigate LFO depicted in time domain characteristics, GWO-Lead-Lag combination is better in terms overshoot (0.0013 *p.u.*) with remarkable settling time (1.8321 *sec*.) under varying load condition. Furthermore, to figure out the overall performance, quantitative analysis is performed among different controller-optimizer sets, which reveals that in terms of minimum fitness value GWO-PI (-34324.77) and GWO-Lead-Lag (-177651.51) combination are identical to other combinations whereas computational time for both is nearby 14 % less than other combinations. It is to be noted that eigenvalue analysis show that GWO tuned Lead-Lag outperforms all other controller-optimizer combinations since it produces highest damping effect (0.2237) and less settling time (1.8321 *sec*.). The eigenvalue analysis and time domain simulation results show the effectiveness of the proposed controllers and their ability to provide good damping of low frequency oscillations.

5.1 Future Scopes

To achieve high efficiency and high reliability of power system, many control strategies based on advanced control theories have been introduced. Model Predictive Control (MPC) is the only practical control method that takes account of system

constraints explicitly and the only advanced control method to have been adopted widely in industry. To the extension of this research work, MPC can be used as controller that usually uses an online optimization in real time to determine control signals. The solution to optimization problem can be formulated with the help of the system model. At each control interval, an optimization algorithm can be justified to determine the system dynamics by computing a sequence of control input values satisfying the control specifications. LFO mitigation for Multi-Machine system can be implemented for the same loading scenario. Advanced Fuzzy Logic based approach for the optimal design of gain parameters for the GUPFC based damping controller can be implemented. The problem of selecting optimized parameter for damping controller can be formulated by optimization problem with some adaptive controller. In future the performance of the proposed GUPFC based damping controller can be compared to phase compensation method.

Bibliography

[1] P. M. Anderson and A. A. Fouad, *Power system control and stability*. John Wiley & Sons, 2008.

[2] A. T. Al-Awami, Y. Abdel-Magid, and M. Abido, "A particle-swarm-based approach of power system stability enhancement with unified power flow controller," *International Journal of Electrical Power & Energy Systems*, vol. 29, no. 3, pp. 251–259, 2007.

[3] H. Wang, W. Du, *et al.*, *Analysis and damping control of power system low-frequency oscillations*. Springer, 2016.

[4] P. W. Sauer and M. Pai, "Power system dynamics and stability," *Urbana*, 1998.

[5] H. Shayeghi, H. Shayanfar, S. Jalilzadeh, and A. Safari, "Design of output feedback upfc controller for damping of electromechanical oscillations using pso," *Energy Conversion and Management*, vol. 50, no. 10, pp. 2554–2561, 2009.

[6] M. Abido, A. Al-Awami, and Y. Abdel-Magid, "Analysis and design of upfc damping stabilizers for power system stability enhancement," in *Industrial Electronics, 2006 IEEE International Symposium on*, vol. 3, pp. 2040–2045, IEEE, 2006.

[7] H. Shayeghi, H. Shayanfar, S. Jalilzadeh, and A. Safari, "Tuning of damping controller for upfc using quantum particle swarm optimizer," *Energy Conversion and Management*, vol. 51, no. 11, pp. 2299–2306, 2010.

[8] A. Keri, A. Mehraban, X. Lombard, A. Eiriachy, and A. Edris, "Unified power flow controller (upfc): modeling and analysis," *IEEE Transactions on Power Delivery*, vol. 14, no. 2, pp. 648–654, 1999.

[9] M. Kothari and N. Tambey, "Unified power flow controller (upfc) based damping controllers for damping low frequency oscillations in a power system," *IE (I) Journal-EL*, vol. 84, pp. 35–41, 2003.

[10] G. Reed, R. Pape, and M. Takeda, "Advantages of voltage sourced converter (vsc) based design concepts for facts and hvdc-link applications," in *Power Engineering Society General Meeting, 2003, IEEE*, vol. 3, pp. 1816–1821, IEEE, 2003.

[11] Y.-H. Song and A. Johns, *Flexible ac transmission systems (FACTS)*. No. 30, IET, 1999.

[12] N. G. Hingorani, "Flexible ac transmission," *IEEE spectrum*, vol. 30, no. 4, pp. 40–45, 1993.

[13] N. Flourentzou, V. G. Agelidis, and G. D. Demetriades, "Vsc-based hvdc power transmission systems: An overview," *IEEE Transactions on power electronics*, vol. 24, no. 3, pp. 592–602, 2009.

[14] L. Gyugyi, "Unified power-flow control concept for flexible ac transmission systems," in *IEE proceedings C (generation, transmission and distribution)*, vol. 139, pp. 323–331, IET, 1992.

[15] N. G. Hingorani, L. Gyugyi, and M. El-Hawary, *Understanding FACTS: concepts and technology of flexible AC transmission systems*, vol. 1. IEEE press New York, 2000.

[16] X.-P. Zhang, E. Handschin, and M. Yao, "Modeling of the generalized unified power flow controller (gupfc) in a nonlinear interior point opf," *IEEE Transactions on Power Systems*, vol. 16, no. 3, pp. 367–373, 2001.

[17] S. P. Hadi, "Dynamic modeling and damping function of gupfc in multi-machine power system," *IPTEK The Journal for Technology and Science*, vol. 22, no. 4, 2011.

[18] M. M. M. Pambudy, S. P. Hadi, and H. R. Ali, "Flower pollination algorithm for optimal control in multi-machine system with gupfc," in *Information Technology and Electrical Engineering (ICITEE), 2014 6th International Conference on*, pp. 1–6, IEEE, 2014.

[19] R. S. Lubis, "Modeling and simulation of generalized unified power flow controller (gupfc)," in *Instrumentation, Communications, Information Technology, and Biomedical Engineering (ICICI-BME), 2011 2nd International Conference on*, pp. 207–213, IEEE, 2011.

[20] D. Valle and P. Araujo, "The influence of gupfc facts device on small signal stability of the electrical power systems," *International Journal of Electrical Power & Energy Systems*, vol. 65, pp. 299–306, 2015.

[21] S. Sharma and S. Vadhera, "Development of generalized unified power flow controller (gupfc) detailed model with a comparison with multi-upfc," *Journal of Information and Optimization Sciences*, vol. 40, no. 2, pp. 233–246, 2019.

[22] R. S. Lubis, "Digital simulation of the generalized unified power flow controller system with 60-pulse gto-based voltage source converter," *Int. J. Electr. Comput. Sci.*, vol. 3, no. 2, pp. 91–6, 2012.

[23] V. Azbe and R. Mihalic, "Damping of power-system oscillations with the application of a gupfc," in *2009 IEEE Bucharest PowerTech*, pp. 1–6, IEEE, 2009.

[24] A. Mohanty, S. Patra, and P. K. Ray, "Robust fuzzy-sliding mode based upfc controller for transient stability analysis in autonomous wind-diesel-pv hybrid system," *IET Generation, Transmission & Distribution*, vol. 10, no. 5, pp. 1248–1257, 2016.

[25] N. G. Hingorani, "High power electronics and flexible ac transmission system," in *Proceedings of the American Power Conference;(USA)*, vol. 50, 1988.

[26] E. Barrios-Martínez and C. Ángeles-Camacho, "Technical comparison of facts controllers in parallel connection," *Journal of applied research and technology*, vol. 15, no. 1, pp. 36–44, 2017.

[27] S. Chirantan, R. Jena, S. Swain, and P. Panda, "Comparative analysis of statcomand tcsc facts controller for power profile enhancement in a long transmission line," in *2017 2nd International Conference on Communication and Electronics Systems (ICCES)*, pp. 407–413, IEEE, 2017.

[28] M. Dogan, S. Tosun, A. Ozturk, and M. K. Dosoglu, "Investigation of tcsc and sssc controller effects on the power system," in *2011 7th International Conference on Electrical and Electronics Engineering (ELECO)*, pp. I–127, IEEE, 2011.

[29] Y. Ye, M. Kazerani, and V. Quintana, "Current-source converter based sssc: modeling and control," in *2001 Power Engineering Society Summer Meeting. Conference Proceedings (Cat. No. 01CH37262)*, vol. 2, pp. 949–954, IEEE, 2001.

[30] H. Wang, "Design of sssc damping controller to improve power system oscillation stability," in *1999 IEEE Africon. 5th Africon Conference in Africa (Cat. No. 99CH36342)*, vol. 1, pp. 495–500, IEEE, 1999.

[31] B. Singh, R. Saha, A. Chandra, and K. Al-Haddad, "Static synchronous compensators (statcom): a review," *IET Power Electronics*, vol. 2, no. 4, pp. 297–324, 2009.

[32] H. Wang, "Phillips–heffron model of power systems installed with statcom and applications," *IEE Proceedings-Generation, Transmission and Distribution*, vol. 146, no. 5, pp. 521–527, 1999.

[33] J. V. Milanovic and Y. Zhang, "Modeling of facts devices for voltage sag mitigation studies in large power systems," *IEEE transactions on power delivery*, vol. 25, no. 4, pp. 3044–3052, 2010.

[34] M. Abido and Y. Abdel-Magid, "Coordinated design of a pss and an svc-based controller to enhance power system stability," *International journal of electrical power & energy systems*, vol. 25, no. 9, pp. 695–704, 2003.

[35] Y.-n. Yu, "Electric power system dynamics.," *ACADEMIC PRESS, INC., 111 FIFTH AVE., NEW YORK, NY 10003, USA, 1983, 256*, 1983.

[36] H. Wang and F. Swift, "A unified model for the analysis of facts devices in damping power system oscillations. i. single-machine infinite-bus power systems," *IEEE Transactions on Power Delivery*, vol. 12, no. 2, pp. 941–946, 1997.

[37] P. Kundur, N. J. Balu, and M. G. Lauby, *Power system stability and control*, vol. 7. McGraw-hill New York, 1994.

[38] K. Padiyar, *Power system dynamics*. BS publications, 2008.

[39] G. Rogers, *Power system oscillations*. Springer Science & Business Media, 2012.

[40] T. Möller, R. Machiraju, K. Mueller, and R. Yagel, "Evaluation and design of filters using a taylor series expansion," 1997.

[41] A. Emadi, "Modeling of power electronic loads in ac distribution systems using the generalized state-space averaging method," *IEEE Transactions on Industrial Electronics*, vol. 51, no. 5, pp. 992–1000, 2004.

[42] C. M. Rimvall and C. P. Jobling, "Computer-aided control system design.," *IEEE Control Systems Magazine*, vol. 13, no. 2, pp. 14–16, 1993.

[43] K. Prasertwong, N. Mithulananthan, and D. Thakur, "Understanding low-frequency oscillation in power systems," *International Journal of Electrical Engineering Education*, vol. 47, no. 3, pp. 248–262, 2010.

[44] C. A. Cañizares, N. Mithulananthan, F. Milano, and J. Reeve, "Linear performance indices to predict oscillatory stability problems in power systems," *IEEE Transactions on Power Systems*, vol. 19, no. 2, pp. 1104–1114, 2004.

[45] M. Gibbard, "Co-ordinated design of multimachine power system stabilisers based on damping torque concepts.," in *IEE Proceedings C (Generation, Transmission and Distribution)*, vol. 135, pp. 276–284, IET, 1988.

[46] N. Bizon, H. Shayeghi, and N. M. Tabatabaei, *Analysis, control and optimal operations in hybrid power systems: Advanced techniques and applications for linear and nonlinear systems*. Springer, 2013.

[47] B. K. Kumar, S. Singh, and S. Srivastava, "Placement of facts controllers using modal controllability indices to damp out power system oscillations," *IET Generation, Transmission & Distribution*, vol. 1, no. 2, pp. 209–217, 2007.

[48] M. E. Aboul-Ela, A. Sallam, J. D. McCalley, and A. Fouad, "Damping controller design for power system oscillations using global signals," *IEEE Transactions on Power Systems*, vol. 11, no. 2, pp. 767–773, 1996.

[49] C.-S. Liu, "An optimally generalized steepest-descent algorithm for solving ill-posed linear systems," *Journal of Applied Mathematics*, vol. 2013, 2013.

[50] S. Mirjalili, S. M. Mirjalili, and A. Lewis, "Grey wolf optimizer," *Advances in engineering software*, vol. 69, pp. 46–61, 2014.

[51] A. Ahmed and M. S. Ullah, "Optimal design of proportional–integral controllers for stand-alone solid oxide fuel cell power plant using differential evolution algorithm," *SpringerPlus*, vol. 5, no. 1, p. 383, 2016.

[52] A. Rezaee Jordehi and J. Jasni, "Parameter selection in particle swarm optimisation: a survey," *Journal of Experimental & Theoretical Artificial Intelligence*, vol. 25, no. 4, pp. 527–542, 2013.

[53] T. Zeugmann, P. Poupart, J. Kennedy, X. Jin, J. Han, L. Saitta, M. Sebag, J. Peters, J. Bagnell, W. Daelemans, *et al.*, "Particle swarm optimization," 2011.

[54] P. ERDOĞMUŞ, "Nature inspired optimization algorithms and their performance on the solution of nonlinear equation systems," *Sakarya University Journal of Computer and Information Sciences*, vol. 1, no. 1, pp. 44–57, 2018.

[55] C. Muro, R. Escobedo, L. Spector, and R. Coppinger, "Wolf-pack (canis lupus) hunting strategies emerge from simple rules in computational simulations," *Behavioural processes*, vol. 88, no. 3, pp. 192–197, 2011.

[56] A. Askarzadeh and A. Rezazadeh, "A new heuristic optimization algorithm for modeling of proton exchange membrane fuel cell: bird mating optimizer," *International Journal of Energy Research*, vol. 37, no. 10, pp. 1196–1204, 2013.

[57] R. Storn and K. Price, "Differential evolution–a simple and efficient heuristic for global optimization over continuous spaces," *Journal of global optimization*, vol. 11, no. 4, pp. 341–359, 1997.

[58] A. Ahmed, M. M. H. Galib, S. M. K. Zaman, and G. Sarowar, "An optimization methodology of susceptance variation using lead-lag controller for grid connected fsig based wind generator system," *Journal of the Franklin Institute*, vol. 355, no. 1, pp. 197–217, 2018.

[59] Y. Abdel-Magid, M. Abido, S. Al-Baiyat, and A. Mantawy, "Simultaneous stabilization of multimachine power systems via genetic algorithms," *IEEE transactions on Power Systems*, vol. 14, no. 4, 1999.

[60] F. Milano, "An open source power system analysis toolbox," *IEEE Transactions on Power systems*, vol. 20, no. 3, pp. 1199–1206, 2005.

[61] F. Milano, "Psat: Power system analysis toolbox, version 2.0. 0-beta," 2007.

[62] D. Lee, "Ieee recommended practice for excitation system models for power system stability studies (ieee std 421.5-1992)," *Energy Development and Power Generating Committee of the Power Engineering Society*, vol. 95, no. 96, 1992.

[63] P. Dalgaard, *Introductory statistics with R*. Springer Science & Business Media, 2008.